Currency Return Dynamics:

What Is the Role of U.S. Macroeconomic Regimes?*

Guanhao Feng Jingyu He Junye Li Lucio Sarno Qianshu Zhang

First Draft: May 2023; This Draft: August 2024

Abstract

This paper examines how changes in U.S. macroeconomic conditions affect the underlying factors that drive currency return dynamics. The study adopts a tree-based Bayesian regime-switching model that identifies shifts in currency return dynamics instrumented by macroeconomic variables. The empirical analysis finds strong evidence of regime changes in the currency risk-return relationship, which are determined interactively by U.S. inflation and interest rates. The Carry factor is identified as a common and dominant factor across all regimes, generating a high risk premium and selection probability, while other factors are regime-specific.

Keywords: Business Cycles; Currency Returns; Decision Tree; Regime Switching; Risk Premia.

JEL Classification: C11, G12, G15.

*We thank Liyuan Cui, Yongmiao Hong, Zhenya Liu (discussant), Qi Xu, Sining Liu (discussant), Yushan Tang (discussant) and seminar and conference participants at the City University of Hong Kong, Zhejiang University, 2024 SoFiE Annual Conference, 2024 China International Conference in Finance, 2024 AsianFA Annual Conference, 2024 Big Data and Econometric Conference (XMU), 2023 Econometric Workshop for Time-varying Coefficient Models (HNU) for their valuable comments. Feng (E-mail: gavin.feng@cityu.edu.hk), He (E-mail: jingyuhe@cityu.edu.hk) and Zhang (E-mail: qszhang7-c@my.cityu.edu.hk) are at City University of Hong Kong; Li (E-mail: li_junye@fudan.edu.cn) is at Fudan University; Sarno (E-mail: l.sarno@jbs.cam.ac.uk) is at University of Cambridge and Centre for Economic Policy Research (CEPR).

1 Introduction

Understanding the currency risk-return relationship is important for optimal exchange rate policy choices. Recent studies show that a small number of common factors can capture the currency return dynamics and explain the cross-sectional variation of currency returns (see, e.g., Chernov, Dahlquist, and Lochstoer, 2023; Nucera, Sarno, and Zinna, 2024; Li, Sarno, and Zinna, 2024). The exchange rates are determined by the relative strength and variation of the macroeconomic fundamentals of the two countries. However, many macroeconomic variables exhibit occasional drastic shifts in behavior linked to events such as financial crises or sudden policy changes (e.g., Stock and Watson, 1996; McConnell and Perez-Quiros, 2000), suggesting that macroeconomic conditions feature regime changes. Therefore, the currency risk-return relationships among regimes may differ, possibly resulting in different factor risk premia, mispricing, and idiosyncratic volatility (e.g., Bekaert, 1995; Johnson, 2002; Gabaix and Maggiori, 2015).

This paper proposes a Bayesian regime-switching model that employs decision trees to uncover currency risk-return relationships within endogenously selected macroeconomic regimes. We assume that currency characteristics capture the dynamics of currency returns, and both mispricing and risk premia are regime-specific and are functions of macro variables defining the regimes (e.g., Kho, 1996; Lettau et al., 2014; Smith and Timmermann, 2022). One crucial problem is how to detect and describe each regime in a parsimonious way using various macro variables explicitly. The goal is achieved by borrowing and customizing the idea of decision trees from machine learning in a Bayesian framework.

Specifically, our model relies on time series information of macro variables, such as interest rates, inflation, and nonfarm payroll, to grow a tree and partition the space of return observations. We exploit the Bayesian spike-and-slab prior[1] to select heterogeneous factor structures and related risk premia for each regime. We modify this

[1] Giannone et al. (2021) also use the same prior when comparing sparse and dense representations in economics and finance.

approach to enable the separate estimation of individual mispricing, heteroskedasticity, and joint estimation of risk premia.[2]

We estimate the risk premia of the selected factors and form regimes iteratively, ensuring that currency factor risk premia are the same within each regime. Our tree-based Bayesian regime-switching model relies on a global split criterion based on the marginal likelihood to assess model fitness to the data. Instead of relying on point estimates of model parameters, which can be inaccurate and prone to overfitting with noisy return data, we adopt a Bayesian approach. We calculate the model's marginal likelihood by integrating out parameters a priori, allowing us to account for parameter and model uncertainties.

Methodology Contributions. The current literature on time series analysis and macroeconomic modeling often emphasizes modeling regime-switching patterns by defining a finite number of regimes and identifying shifts through Markov-switching analysis (e.g., Hamilton, 1989). However, these methods fail to establish connections or similarities between nonadjacent regimes and are often hard to use in high-dimensional modeling. Another approach, named threshold type models, involves detecting regimes based on some variable, but it typically focuses on a single time series at a time.

In contrast, our tree-based Bayesian regime-switching model takes a different approach. It can implicitly define regimes for a large cross-section of assets based on the time series of a set of macro variables and their interactions. For example, we can define currency return regimes based on interest rate or inflation values, even if they are disjoint. This approach provides a more nuanced and accurate understanding of regime changes, facilitating improved forecasting and decision-making in macroeconomic policy analysis. Our model can, therefore, be interpreted as a macro-instrumented regime detection approach. We also show that our model can be generalized to a structural break model when defining regimes based on calendar months.

Empirical Highlights. We collect 49 currencies with respect to the US Dollar and calculate their monthly returns from 1986 to 2023. Since the US economy significantly

[2]Our simulation study validates the effectiveness of this modified approach.

influences global economics, we take the viewpoint of a US investor to study the impact of US macroeconomic conditions on currency excess returns. On one hand, global central banks must closely monitor US macroeconomic conditions and respond to unexpected shocks to stabilize their currency. This proactive approach allows them to consider necessary measures, such as adjusting interest rates, in response to actions taken by institutions like the Federal Reserve. On the other hand, for a US investor in currency markets with many currencies in her well-diversified portfolio, the foreign country-specific risk averages out, and she largely bears the US-specific risk. Lustig, Roussanov, and Verdelhan (2014) find that aggregate returns in currency markets are highly predictable, and US macro variables are powerful predictors determining the time-variation of expected currency returns.

Our study includes 8 key US macroeconomic indicators and 11 currency characteristics to capture the factors affecting currency returns. The indicators include interest rate, inflation, industrial production, nonfarm payroll, unemployment rate, M2, oil price, and VIX. The currency characteristics include Carry trade, short-, medium-, and long-term momentums, value, global imbalances, liabilities in domestic currencies, long-term yields, term spread, currency volatility, and currency market beta.

We summarize our empirical findings as follows. First, our tree-based Bayesian regime-switching model significantly improves the marginal likelihood compared to the model without regime-switching. We identify three regimes based on inflation and interest rates: a high inflation regime, a low inflation and low interest rate regime, and a low inflation and high interest rate regime. Second, currency returns under each regime exhibit different factor structures and different factor risk premia estimates. We find that the Carry factor is a strong factor and consistently generates high risk premia across all regimes, while other factors are weak or uncommon factors, and their risk premia change dramatically across regimes. The factors of NFA and market beta are crucial in the high-inflation regime, the value factor is important in the low inflation and low interest rate regimes, and the volatility factor becomes crucial in the low inflation and high interest rate regime. Third, mispricing and idiosyncratic volatility vary

in time series and cross section, and with comparison to the other regimes, the high inflation regime features relatively high mispricing and idiosyncratic volatility.

Related Literature. The macroeconomic environment undergoes regime changes (e.g., McConnell and Perez-Quiros, 2000; Hamilton, 2016), and investors frequently learn from the historical data, both suggesting that underlying asset pricing models hardly stay stationary over time (e.g., Ang and Bekaert, 2002; Lettau et al., 2008; Lustig et al., 2014). Estimating regime changes has long been a critical issue in the literature. The econometric literature has traditionally relied on regime shift detection based on Markov switching (e.g., Hamilton, 1989), which assumes a finite number of regimes and captures cycles of economic activity around a long-term trend. Another special approach to detect regimes, named structural break, is the change point process considered by Chib (1998) and studied in the context of dynamics in stock returns by (Pástor and Stambaugh, 2001). In this model, the set of regimes expands over time, each regime is unique, and previous regimes are not visited again. A recent paper of Cui et al. (2023) estimates structural breaks for asset pricing factors using conditioning variables as instrumental variables within GMM indirectly. Recently, Smith and Timmermann (2021) utilize cross-sectional information to identify homogeneous structural breaks, and Smith and Timmermann (2022) extend their method to illustrate the changes in factor risk premia across heterogeneous breaks.

Our paper contributes to the threshold-type regime detection model. Threshold regression models are designed to classify observations into different classes based on the value of a specific observed variable (Hansen, 1999, 2000; Hansen and Seo, 2002). The threshold-type regime identification has recently been extended and applied to the factor model (Massacci, 2017; Liu and Chen, 2020; Massacci, 2023). However, these studies only focus on one predetermined state variable and perform hypothesis testing to identify threshold values. Alternatively, our approach selects macroeconomic predictor candidates to split the time dimension more than once and create macro-instrumented regimes that intersect from a Bayesian perspective.

Few currency literature studies account for regime changes when examining cur-

rency risk-return relations. Since Lustig and Verdelhan (2007), the currency literature has documented various profitable currency investment strategies. The most prominent strategies include currency Carry (e.g., Lustig et al., 2011; Menkhoff et al., 2012a; Lettau et al., 2014; Koijen et al., 2018), currency momentum (e.g., Menkhoff et al., 2012b; Asness et al., 2013), and currency value (e.g., Asness et al., 2013; Menkhoff et al., 2017). The literature also finds other profitable strategies that are correlated with these canonical strategies (e.g., Lettau et al., 2014; Della Corte et al., 2016; Colacito et al., 2020; Dahlquist and Hasseltoft, 2020; Fan et al., 2022). A recent study by Nucera, Sarno, and Zinna (2024) using a large cross-section of currency portfolios suggests at least three, possibly four, latent factors in currency returns, which are closely related to the Carry and short-term momentum. In contrast, using only 10 currencies of the developed countries, Chernov, Dahlquist, and Lochstoer (2023) find that Carry and value factors contain significant portions of priced risk, followed by momentum. These divergent findings may stem from a lack of consideration for regime changes in currency markets.

Our paper introduces a novel tree-based Bayesian regime-switching model that combines decision trees and Bayesian methods. The model extends XBART (He et al., 2019; He and Hahn, 2023) by incorporating Bayesian factor risk premia selection, emphasizing detecting macroeconomic regimes. Tree-based machine learning methods have gained wide attention in pricing equity/bond risks for their nonlinear modeling using high-dimensional characteristics (e.g., Gu et al., 2020; Bianchi et al., 2021; Cong et al., 2023). Cong et al. (2023) propose a similar approach to examine asset heterogeneity and select uncommon factor models. Bayesian methods have a long history of applications to empirical asset pricing (e.g., Harvey and Zhou, 1990; Avramov, 2002; Fulop and Li, 2013; Feng and He, 2022; Cimadomo et al., 2022; Bryzgalova et al., 2023). Creal and Kim (2021) explore the risk-return tradeoff in currency returns relying on the Bayesian Additive and Regression Trees (BART) (Chipman et al., 2010), but overlook macroeconomic information and regime changes.

The rest of the paper proceeds as follows. Section 2 presents our tree-based Bayesian

regime-switching model. Section 3 introduces various types of data used in the paper. Section 4 presents our main empirical findings. Section 5 concludes the paper.

2 Methodology

Before proceeding, we first clarify notations. Let $r_{i,t}$ denote the return of currency i at period t. We use individual currency returns in empirical applications, so returns are unbalanced. We assume that $\mathbf{x}_{t-1} = (x_{1,t-1}, \cdots, x_{M,t-1})$ represents a vector of M lagged macro variables, and $\mathbf{Z}_{i,t-1} = (z_{i,1,t-1}, \cdots, z_{i,K,t-1})$ denotes a vector of K currency characteristics of individual currency i that may affect the variation of currency returns. A potential regime is defined as

$$\mathcal{R}_j = \{t \mid \cup_{\text{some } m}\{x_{m,t-1} \leq c_m\} \cup_{\text{some other } m} \{x_{m,t-1} > c_m\}\}, \tag{1}$$

which is a set of periods such that the value of various macro variables $x_{m,t-1}$ (for example, inflation) are smaller (or larger) than a threshold c_m. As discussed in later sections, the number of macro variables defining a regime can be determined using a tree clustering algorithm. These regimes may consist of non-contiguous periods with low or high values of a specific macro variable. In the following, we describe the complete model encompassing all identified regimes, and then introduce the procedures for detecting and estimating regimes.

2.1 Full Model with All Regimes

Suppose there are $j = 1, \cdots, J$ regimes on the time horizon. The model is given by

$$r_{i,t} = \boldsymbol{\alpha}(\mathbf{x}_{t-1}) + \boldsymbol{\lambda}(\mathbf{x}_{t-1})^{\mathsf{T}}\mathbf{Z}_{i,t-1} + \epsilon_{i,t} \tag{2}$$

where

$$\boldsymbol{\alpha}(\mathbf{x}_{t-1}) = \sum_{j=1}^{J} \mathbb{1}_{\{t\in\mathcal{R}_j\}}\alpha_{j,i}, \qquad \boldsymbol{\lambda}(\mathbf{x}_{t-1}) = \sum_{j=1}^{J} \mathbb{1}_{\{t\in\mathcal{R}_j\}}\boldsymbol{\lambda}_j,$$
$$\epsilon_{i,t} \overset{\text{independent}}{\sim} N(0,\sigma_{i,t}^2), \qquad \sigma_{i,t}^2 = \sum_{j=1}^{J} \mathbb{1}_{\{t\in\mathcal{R}_j\}}\sigma_{j,i}^2.$$

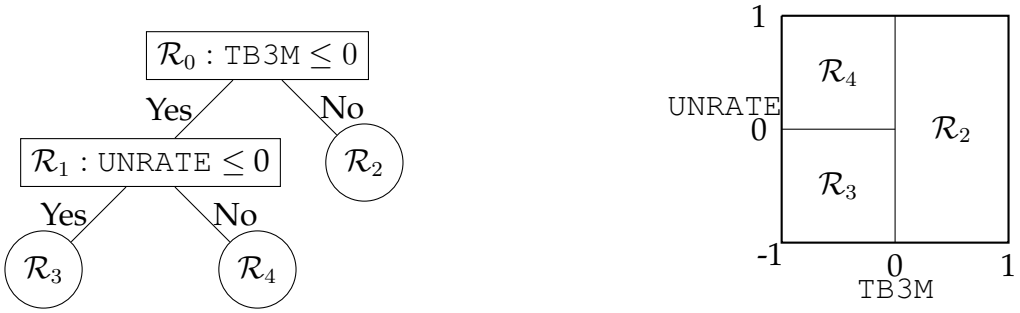
The indicator function, $\mathbb{1}_{\{t\in\mathcal{R}_j\}}$, checks whether the t-th time period is in regime $\mathcal{R}_j$ or not, and the time period t belongs to one and only one regime. $\mathbf{Z}_{i,t-1}$ is the lagged currency characteristics for currency i at time $t-1$. As in Fama and French (2020) and Smith and Timmermann (2022), the coefficient vector $\boldsymbol{\lambda}_j$ consists of K elements and can be interpreted as factor risk premia with pre-specified time-varying factor loadings (characteristics). We designate $\boldsymbol{\alpha}$, $\boldsymbol{\sigma}$ and $\boldsymbol{\lambda}$ as regime-specific parameters, enabling the incorporation of diverse currency return patterns over the time horizon. These parameters are dynamic and depend on macro variables, defining the regimes by aggregating indicator functions.

Efficiently identifying and characterizing each regime using macro variables poses a challenge. To overcome this challenge, we leverage the concept of trees from machine learning combined with a traditional threshold-type model. Figure 1 provides a straightforward example that demonstrates the definition of three regimes based on macro variables, including interest rate and unemployment rate. Following binary split rules from the top node and navigating through left or right subnodes based on rule satisfaction, we can sequentially trace the tree path to identify the corresponding bottom nodes representing the different regimes. For instance, regime $\mathcal{R}4$ can be described as $\mathcal{R}4 = \{t \mid \texttt{TB3M}_{t-1} \leq 0 \text{ and } \texttt{UNRATE}_{t-1} > 0\}$, with the other two regimes following a similar pattern, where the two macro variables are normalized to be between -1 and 1.

The tree structure is represented as a function of macro variables $\mathcal{T}(\mathbf{x}_{t-1})$, which takes the value of a vector comprising all macro variables at period $t-1$ and provides the corresponding regime label. Importantly, this function returns only one label, ensuring no regime overlap. Considering a multi-way split at each node is unnecessary

Figure 1: **A Decision Tree Describing Regimes by Macro Variables.**

Left: A decision tree with two splits and three leaves. Right: Corresponding partition plot for the macro variable space spanned by TB3M and UNRATE, resulting in three distinct regimes labeled as $\mathcal{R}_3$, $\mathcal{R}_4$, $\mathcal{R}_5$. Both TB3M and UNRATE are normalized to be in $[-1, 1]$.



since sequential binary splits can equivalently represent it. In the subsequent discussion, we interpret $\texttt{TB3M}_{t-1} \leq 0$ as a split rule, with 0 as the split value.

So far, the number of regimes and split rules are fixed. The next section will introduce a modified panel regression model with Bayesian spike-and-slab priors for factor risk premia selection within each regime. Additionally, an algorithm will be presented to detect regimes and select factors within each regime.

2.2 Bayesian Variable Selection and Marginal Likelihood

For each regime j and individual currency i, plugging the dynamics of $\boldsymbol{\alpha}$ and $\boldsymbol{\lambda}$ into the model of currency returns yields

$$r_{i,t} = \alpha_{j,i} + \boldsymbol{\lambda}_j^\top \mathbf{Z}_{i,t-1} + \epsilon_{i,t}. \tag{3}$$

We select the risk premia of factors among each regime's $\boldsymbol{\lambda}_j$ using the Bayesian spike-and-slab priors (George and McCulloch, 1993). The prior distributions of all coefficients are as follows:

$$\begin{aligned}
&\pi(\lambda_{j,k} \mid \boldsymbol{\gamma}_j) = (1-\gamma_{j,k})N(0, \xi_0^2) + \gamma_{j,k} N(0, \xi_1^2), \\
&\pi(\alpha_{j,i} \mid \sigma_{j,i}^2) = N(0, \sigma_\alpha^2 \sigma_{j,i}^2), \\
&\pi(\sigma_{j,i}^2) = \text{inverse-Gamma}(v_0, S_0), \\
&\pi(\boldsymbol{\gamma}_j) = \prod_{k=1}^{K} w_k^{\gamma_{j,k}} (1-w_k)^{(1-\gamma_{j,k})}.
\end{aligned} \tag{4}$$

We employ a spike-and-slab prior, a mixture of normal and different prior variances. The latent dummy variables $\boldsymbol{\gamma}_j = (\gamma_{j,1}, \cdots, \gamma_{j,K})$ play a crucial role in this framework. Each $\gamma_{j,k}$ takes a value of 1 or 0, indicating whether the prior for the corresponding coefficient $\lambda_{j,k}$ belongs to the slab or the spike. If $\gamma_{j,k} = 1$, it signifies the selection of the corresponding factor risk premia λ and assigns a large value of ξ_1 to the slab, resulting in less shrinkage of the coefficients. On the other hand, when $\gamma_{j,k} = 0$, it implies that factor risk premia λ_k is not included, and the corresponding coefficient $\lambda_{j,k}$ are shrunk towards zero within the spike component, which is characterized by a small value of ξ_0. Traditional spike-and-slab prior only applies to variable selection on a single time series. We modify it to estimate the pooled regression model, where the risk premia estimate (the slope coefficient) is the same across the cross section, and different alphas and heteroskedasticity are allowed for individual currencies.

To capture the investor's prior belief regarding each factor's risk premium, a hyper-parameter w_k is chosen. This paper discusses three types of investors: a confident investor with $w_k = 0.9$ who finds most factors useful; an agnostic investor with $w_k = 0.5$ who is indifferent towards all factors; and a skeptic investor with $w_k = 0.1$ who believes each factor has a 10 % chance of being included in the model.

We measure model fitness to evaluate the performance of our regime-switching model on the data. Unlike the frequentist approach that relies on calculating the sum of squared residual errors of the model of Equation (3) using point estimates of $\alpha_{j,i}$ and $\boldsymbol{\lambda}_j$, which can be sensitive to noisy data, we take a Bayesian perspective. Instead, we compute the model's marginal likelihood by integrating out the parameters, thereby accounting for the uncertainty in parameter estimates. This Bayesian approach allows us to consider the variability in parameter estimation, improve the accuracy of model predictions, and effectively address the issue of over-fitting.

Notice that each regime contains only a subset of time periods. We stack all the data of currency returns for individual currencies and risk factors within the j-th regime in a matrix form, $\mathbf{R}_{j,i}$ and $\mathbf{Z}_{j,i}$, respectively. Because of the independence of residuals, the marginal likelihood of the model at any regime $\mathcal{R}_j$ is given by the

product of individual marginal likelihood:

$$p(\mathcal{R}_j) := \prod_i p(\mathbf{R}_{j,i} \mid \mathbf{Z}_{j,i}) = \prod_i \int p(\mathbf{R}_{j,i} \mid \mathbf{Z}_{j,i}, \boldsymbol{\gamma}_j, \alpha_{j,i}, \boldsymbol{\lambda}_j, \sigma^2_{j,i}) \\ \times \pi(\alpha_{j,i} \mid \sigma^2_{j,i}) \pi(\boldsymbol{\lambda}_j \mid \boldsymbol{\gamma}_j) \pi(\sigma^2_{j,i} \mid \boldsymbol{\gamma}_j) \pi(\boldsymbol{\gamma}_j) d\alpha_{j,i} d\boldsymbol{\lambda}_j d\sigma^2_{j,i} d\boldsymbol{\gamma}_j. \tag{5}$$

The marginal likelihood incorporates the expectations of unknown parameters in the likelihood function, by considering the prior distributions. Doing so encompasses parameter estimation and model selection uncertainties, which depend solely on the data and prior parameters. Utilizing the marginal likelihood enables the separation of regime detection and parameter estimation procedures.

However, the marginal likelihood in Equation (5) lacks a closed-form representation. Therefore, we follow Chib (1995) to calculate the marginal likelihood numerically using posterior samples drawn from the corresponding Gibbs sampler.

See the Appendix A.I for detailed derivations. In the following sections, to simplify notations, we denote $p(\mathcal{R}_0)$ as the marginal likelihood evaluation of Equation (5) conditional on the data within regime $\mathcal{R}_0$.

2.3 Macro-Instrumented Regime Detection

In this section, we introduce our Bayesian regime-switching approach, a customized tree growth algorithm for partitioning currency return data based on the fitness of the factor risk premia selection model. The tree, depicted in Figure 1, divides the time horizon into regimes using macroeconomic variables. The algorithm starts with the initial split at node $\mathcal{R}_0$ and grows the tree top-down, creating child nodes representing distinct time series regimes. This process continues by jointly splitting each child node until some specific stopping conditions are met. During each step, our approach evaluates all potential split rules using the marginal likelihood of the model Equation (5), selecting the rule that yields the highest gain.

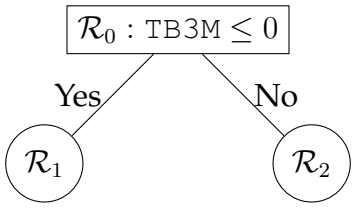
To find the initial split, we assess all potential split rule candidates, which consist of pairs of macro variables and corresponding cut values to divide the currency return time series. Figure 2 shows an example of such a candidate split. Each pair of a macro

variable and the corresponding cut value generates distinct regimes, denoted as $\mathcal{R}_1$ and $\mathcal{R}_2$. The crucial question arises: which regime should be chosen?

To tackle this issue, we assess the effectiveness of the risk premia selection model presented in Equation (2). We aim to identify a split rule that maximizes the overall gain in model fitness. To accomplish this, we quantitatively evaluate the marginal likelihood outlined in Equation (5), enabling us to determine the optimal split rule.

Figure 2: **Illustration of one candidate for the first split**

To calculate the split criterion and identify the optimal cutpoint, let's examine one potential split candidate: $\texttt{TB3M} \leq 0$. $\texttt{TB3M}$ is normalized to be in $[-1, 1]$.



Suppose $\mathcal{C} = \tilde{c}_j$ is the set of all split rule candidates. To simplify the calculation, we evaluate only one possible cut value for each macro variable, 0, allowing for two possible regimes. Because we will demean all the variables in a previous 10-year rolling window, the cut point of 0 represents whether the macro variable has been at a high or low level over the past decade. Each of them partitions the root node, $\mathcal{R}_0$, into two child leaf nodes (as illustrated in Figure 2). Since $\epsilon_{i,t}$'s are assumed independent, the joint marginal likelihood of the complete dataset of currency returns is the product of the marginal likelihood for the two child nodes

$$l(c_j) = p(\mathcal{R}_1) \times p(\mathcal{R}_2) = p(\mathbf{R}^L \mid \mathbf{Z}^L) \times p(\mathbf{R}^R \mid \mathbf{Z}^R), \tag{6}$$

where the superscripts L and R indicate data observations from the left and right child nodes. Each split rule has a different data partition, and the evaluation of Equation (6) varies, with a large value indicating better overall model fit after the partition. Therefore, it is a natural measurement of a candidate, which we call the split criterion. Please refer to the appendix A.II for further split and stop criterion.

The tree grows consistently for all future splits. At each split (j-th split), we eval-

uate the global split criterion and stop option for all existing leaf nodes. The candidate that optimizes the criterion is selected. The algorithm continues until the stop option is chosen or certain predetermined stop conditions are satisfied, such as reaching a minimum number of data in a leaf node or the maximum depth. After $J-1$ iterations, the algorithm concludes and results in J regimes.

After growing the trees using marginal likelihood to address parameter uncertainty, we explore the posterior distribution of parameters. Each leaf node obtained from the tree growth algorithm represents a specific regime in the time series. Subsequently, we fit the Bayesian leaf model in Equation (3) for each regime and draw posterior samples using the Gibbs sampler, which is presented next.

2.4 Gibbs sampler

The posterior inference of parameters for the factor model within each regime is achieved by Markov chain Monte Carlo (MCMC) and a Gibbs sampler. Here, we utilize a modified spike-and-slab prior for the pooled regression model. We estimate mispricing and idiosyncratic variance for each currency, then jointly estimate factor risk premia selection. Expressing the stacked data within regime j of individual currency portfolio i ($1 \leq i \leq N$) in matrix form $\mathbf{R}_{j,i}$ and $\mathbf{Z}_{j,i}$, we have

$$\mathbf{R}_{j,i} = \alpha_{j,i} + \mathbf{Z}_{j,i}\boldsymbol{\lambda}_j + \boldsymbol{\epsilon}_{j,i}, \tag{7}$$

the full conditionals are given as follows,

1. Update $\alpha_{j,i}$. Different from the slope coefficient λ_j, the intercept differs across individual currencies, indicating different levels of individual mispricing. For each j and $i = 1, ..., N$,

$$\alpha_{j,i}|\boldsymbol{\lambda_j}, \sigma^2_{j,i}, \boldsymbol{\gamma}_j, \mathbf{R}_{j,i}, \mathbf{Z}_{j,i} \sim \mathcal{N}\left(\tilde{\alpha}_{j,i}, \frac{\sigma^2_{j,i}}{\mu_{\alpha,j,i}}\right)$$

   where $\mu_{\alpha,j,i} = \mathbf{1}^T\mathbf{1} + \frac{1}{\sigma^2_\alpha}$ and $\tilde{\alpha}_{j,i} = \mu^{-1}_{\alpha,j,i}\mathbf{1}^\mathsf{T}(\mathbf{R}_{j,i} - \mathbf{Z}_{j,i}\boldsymbol{\lambda}_j)$.

2. Update $\boldsymbol{\lambda}_j = \{\lambda_{j,k}\}_{k=1,\cdots,K}$. Note that this step updates the regression coefficients

of all variables. For $i = 1, ..., N$, $k = 1, 2, \cdots, K$,

$$\boldsymbol{\lambda}_j \mid \alpha_{j,i}, \sigma^2_{j,i}, \boldsymbol{\gamma}_j, \mathbf{R}_{j,i}, \mathbf{Z}_{j,i} \sim \mathcal{N}\left(\tilde{\boldsymbol{\lambda}}_j, \boldsymbol{V}_{\lambda,j}\right),$$

where $\boldsymbol{V}_{\lambda,j} = \left(\sum_{i=1}^{N} \sigma^{-2}_{j,i} \mathbf{Z}^T_{j,i} \mathbf{Z}_{j,i} + V_0^{-1}\right)^{-1}$ and $\tilde{\boldsymbol{\lambda}}_j = \boldsymbol{V}_{\lambda,j}\left(\sum_{i=1}^{N} \sigma^{-2}_{j,i} \mathbf{Z}^T_{j,i} \left(\mathbf{R}_{j,i} - \alpha_{j,i}\mathbf{1}\right)\right)$, where V_0^{-1} is a diagonal matrix where the corresponding k-th diagonal element is $\xi^2_{\gamma,k}$.

3. Update $\boldsymbol{\gamma}_{j,k}$, for $k = 1, 2, \cdots, K$.

$$\gamma_{j,k} \mid \boldsymbol{\lambda}_j, \mathbf{R}_j, \mathbf{Z}_j \sim \text{BER}\left(\frac{\xi_1^{-1} \exp\left(-\frac{1}{2\xi_1^2}\lambda^2_{j,k}\right) w_k}{\xi_1^{-1} \exp\left(-\frac{1}{2\xi_1^2}\lambda^2_{j,k}\right) w_k + \xi_0^{-1} \exp\left(-\frac{1}{2\xi_0^2}\lambda^2_{j,k}\right)(1 - w_k)}\right).$$

4. Update $\sigma^2_{j,i}$, for $i = 1, ..., N$

$$\sigma^2_{j,i} \mid \alpha_{j,i}, \boldsymbol{\lambda}_j, \boldsymbol{\gamma}_j, \mathbf{R}_{j,i}, \mathbf{Z}_{j,i} \sim IG(v_i^*, S_i^*),$$

where $v_i^* = \frac{1}{2}(T_i + 1 + v_0)$, $S_i^* = \frac{1}{2}\left(||\mathbf{R}_{j,i} - \alpha_{j,i} - \mathbf{Z}_{j,i}\boldsymbol{\lambda}_{j,i}||_2^2 + \frac{\alpha^2_{j,i}}{\sigma^2_\alpha} + S_0\right)$, and T_i is number of data observations for i-th currency in the leaf node.

In the Internet Appendix, we conduct a simulation study to test the validity of our method. We consider the presence of the three types of factors: strong factors, weak factors, and useless factors, where the strong factors have large risk premia, the weak factors have smaller risk premia, and the useless factors have no risk premia when generating data. The simulation results show that our methodology can effectively identify the three types of factors through sampling. The selection probabilities for the strong factors consistently concentrate around 1, varying between 0 and 1 for the weak factors; however, the useless factors are consistently unselected with very low selection probabilities close to 0. See Section IA.I in the Internet Appendix for all implementation details.

3 Data

This section introduces various types of data used for our empirical analysis, including exchange rates, currency returns, currency characteristics, and leading US macroeconomic variables for regime detection. The sample covers the period from January 1986 to December 2023.

3.1 Exchange Rates and Currency Returns

We collect spot and one-month forward exchange rates with respect to the US dollar (USD) for the following 49 currencies: Australia, Austria, Belgium, Brazil, Bulgaria, Canada, Croatia, Cyprus, Czech Republic, Denmark, Egypt, euro area, Finland, France, Germany, Greece, Hong Kong, Hungary, Iceland, India, Indonesia, Ireland, Israel, Italy, Japan, Kuwait, Malaysia, Mexico, Netherlands, New Zealand, Norway, Philippines, Poland, Portugal, Russia, Saudi Arabia, Singapore, Slovakia, Slovenia, South Africa, South Korea, Spain, Sweden, Switzerland, Taiwan, Thailand, Ukraine, the United Kingdom, and Turkey. The data are from Barclays Bank International (BBI) and WM/Reuters via *Datastream*. We include the Euro series from January 1999 onwards and exclude the euro area countries, keeping only the euro series.

As per standard practice in the literature, we exclude observations during periods of significant CIP failures for a specific currency (see, e.g., Nucera, Sarno, and Zinna, 2024, and references therein): Egypt (01/01/2011 to 30/08/2013; 03/10/2016 to 28/02/2017); Indonesia (01/12/1997 to 31/07/1998; 01/02/2001 to 31/05/2005); Malaysia (01/05/1998 to 30/06/2005); Russia (01/12/2008 to 30/01/2009; 03/11/2014 to 27/02/2015); South Africa (01/08/1985 to 30/08/1985; 01/01/2002 to 31/05/2005); Turkey (01/11/2000 to 30/11/2001); and Ukraine (03/11/2014 to 31/12/2017). From a US investor's perspective, the exchange rate is defined as units of USD per unit of foreign currency (FCU), i.e., USD/FCU. Therefore, an increase in spot and forward rates indicates an appreciation of the foreign currency or a depreciation of the US dollar.

The asset pricing analysis is implemented at a monthly frequency. We compute currency excess returns by sampling end-of-month spot and forward exchange rates.

The excess return on buying a foreign currency in the forward market at month t and then selling it in the spot market at month $t+1$ is defined as,

$$rx_{i,t+1} = \frac{S_{i,t+1} - F_{i,t}}{S_{i,t}}, \tag{8}$$

where $S_{i,t}$ and $F_{i,t}$ are spot and forward rates, respectively, at month t for currency i. The excess return can be decomposed into its spot-return and forward-premium components as follows

$$rx_{i,t+1} = \frac{S_{i,t+1} - S_{i,t}}{S_{i,t}} + \frac{S_{i,t} - F_{i,t}}{S_{i,t}} \approx r_{i,t+1} + \big(i_{i,t} - i_t\big), \tag{9}$$

where $r_{i,t+1}$ is the spot exchange rate return, and $i_{i,t}$ and i_t are the foreign and U.S. dollar interest rates, respectively. The approximation in Equation (9) holds because we follow the common practice of using forward rates rather than interest rate differentials to compute excess returns, i.e., $fp_{i,t} \equiv \frac{S_{i,t}-F_{i,t}}{S_{i,t}} \approx i_{i,t} - i_t$ under covered interest rate parity (CIP).

3.2 Currency Characteristics

Following the literature, we construct various currency characteristics. We consider Carry (e.g., Lustig et al., 2011; Menkhoff et al., 2012a; Lettau et al., 2014; Koijen et al., 2018), short (1-month)-, medium (6-month)-, and long (12-month)-term currency momentum (e.g., Menkhoff et al., 2012b; Asness et al., 2013), currency value (e.g., Asness et al., 2013; Menkhoff et al., 2017), global imbalances based on net foreign assets and liabilities in domestic currencies (Della Corte et al., 2016), long-term yields (Ang and Chen, 2010; Della Corte et al., 2016), term spread (Lustig et al., 2019), currency volatility (Menkhoff et al., 2012a), and currency market beta (Lettau et al., 2014). See Table IA.2 in the Internet Appendix for variable definitions.

To make currency characteristics comparable in the cross section, in each month, we rank all characteristics cross-sectionally and normalize the rank scale in the range of [-1, 1], with their cross-sectional median of 0. Any missing values are then imputed

Table 1: **Summary Statistics**

The table shows summary statistics for 11 currency characteristics and the currency excess return, including the number of non-NaN values, mean, standard deviation, median, 10th percentile, and 90th percentile. There are 11 currency characteristics, whose definitions are provided in Table IA.2. The sample spans over the period from January 1986 to December 2023.

	Num	Mean	Std	Med	p10	p90
Excess Return (%)	12592	-0.17	4.81	0.07	-3.36	3.49
Carry (%)	12592	-0.07	3.03	0.05	-0.20	0.61
MOM1 (%)	12550	-0.17	4.76	0.06	-3.36	3.49
MOM6 (%)	12338	0.14	11.24	0.34	-8.35	9.98
MOM12 (%)	12081	1.06	14.76	0.54	-11.88	16.14
Value	12580	-0.24	0.54	-0.15	-0.68	0.16
NFA	12582	-0.16	1.14	0.12	-1.36	0.58
LDC (million)	12582	96.28	708.66	2.71	0.17	66.57
Long-term Yield	10450	5.38	3.66	4.87	1.27	9.90
Term Spread	9117	0.83	1.71	0.86	-1.00	2.68
Volatility	12592	0.01	0.03	0.01	0.00	0.02
MKT Beta	11822	1.00	0.90	1.10	0.01	1.88

to be 0. One advantage of using the cross-sectional ranks of characteristics is that the impact of potential data errors and outliers in individual characteristics can be largely alleviated (see, e.g., Kelly, Pruitt, and Su, 2019; Freyberger, Neuhierl, and Weber, 2020; Kozak, Nagel, and Santosh, 2020).

Table 1 presents the summary statistics of currency excess returns and 11 characteristics. The table includes the number of observations (Num), mean, standard deviation (Std), median (Med), and 10th and 90th percentiles for each variable. We see that the pooled currency excess return has an average of -0.17% with a standard deviation of 4.81%, and its 10th and 90th percentiles are -3.36% and 3.49%, respectively.

3.3 US Macroeconomic Variables

We employ eight leading US macroeconomic indicators to define the major economic regimes. These macro variables encompass the 3-month interest rate, inflation, industrial production, nonfarm payroll, unemployment rate, M2, crude oil price index, and VIX. Figure IA.1 in the Internet Appendix illustrates the time series of these macroeconomic variables, superimposed by the NBER recessions for reference. Clear

patterns of structural breaks emerge in numerous macroeconomic time series during both boom and recession periods. This paper aims to investigate the underlying macro-instrumented regime-switching behaviors in currency markets.

We demean these macro indicators each time by subtracting the previous 10-year rolling window average. Then, we use a previous 12-month smoothing to make the changes in the macro variables less volatile. If the value of a macro variable is greater than 0, it is higher than the average of the past ten years. For instance, if the interest rate value exceeds 0, the current interest rate level is higher than the average of the observations from the past ten years, signifying a high interest rate regime in the economy. This standardized approach ensures that each predictor's performance is evaluated on a consistent variation scale and is essential for the tree clusters' development in identifying macroeconomic regimes using the recent data.

4 Empirical Results

This section presents our key empirical findings. First, we evaluate the risk premia selection without regime shifts in Subsection 4.1. Then, we examine the marginal likelihood gains and the final tree structure in Subsection 4.2. Next, in Subsection 4.3, we delve into the macroeconomic regimes and the regime-specific risk premia selection. In Subsection 4.4, we examine the cross-sectional mispricing and heteroskedasticity. Finally, Subsection 4.5 connects our model to structural break.

4.1 Full Sample Risk Premia Selection

Before analyzing regime detection, we will examine the entire sample's overall performance without considering any regime shifts, assuming only one regime. In Section 2.4, we use a modified Gibbs Sampler to analyze an eleven-factor model ob-

tained by regressing currency-level excess returns on an intercept and factors.

$$
\begin{aligned}
r_{i,t} \quad = \quad & \alpha_{i,t} + r_{z,t} + \lambda_{Carry} * Carry_{i,t-1} + \lambda_{MOM1} * MOM1_{i,t-1} + \lambda_{MOM6} * MOM6_{i,t-1} \\
& + \lambda_{MOM12} * MOM12_{i,t-1} + \lambda_{Value} * Value_{i,t-1} + \lambda_{NFA} * NFA_{i,t-1} \\
& + \lambda_{LDC} * LDC_{i,t-1} + \lambda_{LT_Yield} * LT_Yield_{i,t-1} + \lambda_{Term_Spread} * Term_Spread_{i,t-1} \\
& + \lambda_{Volatility} * Volatility_{i,t-1} + \lambda_{MKT_Beta} * MKT_Beta_{i,t-1} + \epsilon_{i,t}, \qquad (10)
\end{aligned}
$$

where to ensure residuals among currencies are uncorrelated, we include a common factor $r_{z,t}$ to capture the variation across the cross-section, similar to Pesaran (2006) and Smith and Timmermann (2022). Empirically, we cross-sectionally demean currency excess returns.

We present posterior factor selection probabilities and posterior means of factor risk premia with 5% and 95% credible intervals in the parentheses, calculated using Bayesian Model Averaging (BMA) across the entire set of models. We conduct and report the posterior evaluation over a broad range of the parameter w (as defined in equation (4)), which governs the degree of shrinkage for potentially useless factors. This parameter affects the prior belief on the total fraction of factors that should be included in the model. The results are presented for three types of priors: a confident prior (w = 0.9), an agnostic prior (w = 0.5), and a skeptical prior (w = 0.1). The results in table 2 are presented for these selection economic priors, with the risk premia estimates shown in the left panel and the selection probabilities in the right panel.

Notably, the factors of Carry, market beta, and NFA exhibit statistically significant and economically substantial risk premia and almost 100% selection probabilities for all three types of priors, suggesting that they are strong factors in the entire cross-section of currency returns. This finding differs from those in Nucera, Sarno, and Zinna (2024) and Chernov, Dahlquist, and Lochstoer (2023). Using a large cross-section of currency portfolios, Nucera, Sarno, and Zinna (2024) find at least three, possibly four, latent factors, which dominantly capture the Carry and short-term momentum factors; in contrast, using only 10 individual currencies of the developed countries,

Table 2: **Factor Risk Premia and Selection Probabilities without Regimes**

The table displays risk premia estimation and selection results with no regime shifts. Risk premia estimate and selection probability are presented based on prior selection probability (with $w = 0.9$, $w = 0.5$, and $w = 0.1$). The left panel shows the results of the risk premia estimate (with 5 % and 95 % credible intervals in the parentheses), while the right panel presents the results of the corresponding selection probability. The number is the mean (5 % and 95 % quantiles in the parentheses) of 2000 MCMC post-convergence samples of λ and γ.

	Risk Premia (%)			Selection Probability (%)		
Factors	$w = 0.9$	$w = 0.5$	$w = 0.1$	$w = 0.9$	$w = 0.5$	$w = 0.1$
Carry	0.449 [0.37, 0.53]	0.464 [0.38, 0.54]	0.477 [0.40, 0.55]	100	100	100
MOM1	0.125 [0.04, 0.20]	0.101 [0.02, 0.19]	0.078 [0.02, 0.19]	90	61	24
MOM6	0.196 [0.10, 0.29]	0.162 [0.03, 0.28]	0.075 [0.01, 0.21]	98	79	21
MOM12	-0.149 [-0.23, -0.05]	-0.111 [-0.23, -0.01]	-0.033 [-0.10, 0.02]	94	60	5
Value	0.074 [0.01, 0.14]	0.051 [0.00, 0.11]	0.041 [0.00, 0.08]	71	21	2
NFA	0.256 [0.18, 0.33]	0.239 [0.17, 0.30]	0.228 [0.16, 0.29]	100	100	99
LDC	0.000 [-0.05, 0.06]	-0.001 [-0.04, 0.04]	0.000 [-0.04, 0.04]	34	4	0
LT Yield	0.102 [0.01, 0.19]	0.060 [-0.00, 0.16]	0.042 [-0.00, 0.09]	81	29	5
Term Spread	-0.018 [-0.08, 0.03]	-0.014 [-0.06, 0.03]	-0.013 [-0.05, 0.03]	35	5	0
Volatility	0.042 [-0.01, 0.11]	0.032 [-0.01, 0.08]	0.027 [-0.01, 0.07]	47	10	1
MKT_Beta	0.276 [0.21, 0.34]	0.271 [0.20, 0.33]	0.264 [0.20, 0.33]	100	100	100

Chernov, Dahlquist, and Lochstoer (2023) find that the Carry and value factors contain significant portions of priced risk, followed by momentum.

When we have a confident prior, the factors of MOM1 and MOM6 have statistically significant positive risk premia and high selection probabilities. In contrast, when we become more and more skeptical, their risk premia decrease, and their selection probabilities reduce dramatically. In addition, while the value factor generates a statistically significant positive risk premium for each prior, it is relatively small with

Table 3: **Cross Sectional Alpha and Volatility Estimation with No Regime**

The table displays cross-sectional alpha and volatility distribution with no regime shifts. The top panel shows results of cross-sectional alpha distribution, while the right panel presents cross-sectional σ results. It includes the cross-sectional average and standard deviation of the posterior mean of α and σ estimates, calculated from 2000 MCMC post-convergence samples and different percentiles.

	Prior	Mean	Std	5%	10%	25%	Median	75%	90%	95%
Alpha (%)	w = 0.9	-0.093	1.478	-0.150	-0.092	-0.010	0.090	0.260	0.364	0.410
	w = 0.5	-0.090	1.482	-0.132	-0.092	0.000	0.080	0.270	0.356	0.420
	w = 0.1	-0.089	1.475	-0.130	-0.092	0.000	0.080	0.270	0.356	0.422
Volatility	w = 0.9	2.707	2.934	1.326	1.470	1.640	2.050	2.680	3.636	4.532
	w = 0.5	2.708	2.934	1.330	1.478	1.640	2.050	2.680	3.634	4.528
	w = 0.1	2.709	2.938	1.334	1.466	1.640	2.050	2.680	3.638	4.522

a low selection probability. These findings may suggest that the short-term momentum factor and the value factor are weak factors in the entire cross-section of currency returns. Different from Menkhoff et al. (2012a), the factor risk premium of volatility is not statistically significant, with a very low selection probability for each prior.

To gain insight into mispricing and idiosyncratic volatility in the cross section, Table 3 provides a detailed summary of the cross-sectional mispricing (α) and volatility (σ) distributions for the full sample period from January 1986 to December 2023, without considering any regime shifts. For various priors, the means of alpha hover around -0.10%, exhibiting variability in the cross section with a standard deviation of approximately 1.47%. The alpha percentiles reveal a negative lower end (around 0.14%), a slightly positive median (0.08%), and a positive upper end (0.40%). The cross-sectional means and standard deviations of idiosyncratic volatility are almost the same across different priors, around 2.7%. The percentiles indicate a wide spread from a lower bound of about 1.33% to an upper bound of about 4.53%, with a median of about 2.05%. In summary, alpha and idiosyncratic volatility are consistently estimated regardless of prior beliefs on how likely a factor could be selected.

4.2 Tree Growth and Regime Detection

Importantly, our tree-based Bayesian regime-switching model can identify time-series regimes by iteratively dividing the entire sample universe using US macro variables, guided by marginal likelihood improvements. This enables us to understand how factor risk premia changes concerning macroeconomic conditions.

In the regime-switching literature, the number of regimes is usually selected to 2 or 3 for ease of interpretability. Therefore, we limit the maximum number of splits to two, allowing for three distinct macro-instrumented regimes in our implementation. Figure 3 presents the tree growth process and ultimately detected regimes. The regime classification uses the entire sample from January 1986 to December 2023 and selects the most relevant factors to the cross-sectional variation of currency returns for each regime. It turns out that inflation (CPI) and the 3-month interest rate (TB3M) are the two most important macro variables that define the regimes. The tree algorithm first splits the entire sample based on the inflation rate (CPI) into the high- and low-inflation periods, and further splits the low-inflation periods based on the interest rates into the low- and high-rate periods, resulting in three regimes in the end,

- High inflation regime (Regime 1): CPI > 0;
- Low inflation and low interest rate regime (Regime 2): CPI < 0 and TB3M < 0;
- Low inflation and high interest rate regime (Regime 3): CPI < 0 and TB3M > 0.

Further splitting is possible, but interpreting regimes becomes challenging. The number of months in each regime is also shown in Figure 3: 160 months in Regime 1, 281 months in Regime 2, and only 15 months in Regime 3. The samples in individual regimes are then used to select regime-specific factors and estimate their risk premia.

Figure 4 presents the time-series regime-switching pattern. Regime 1 primarily spans the periods of 1990 to 1992, 2000 to 2002,2005 to 2007,2017 to 2020, and 2021 to 2023; Regime 2 the periods of 1986 to 1990,1992 to 2000, 2002 to 2004, 2009 to 2017, and 2020 to 2021; and Regime 3 the remaining periods. We note that Regime 1 (high

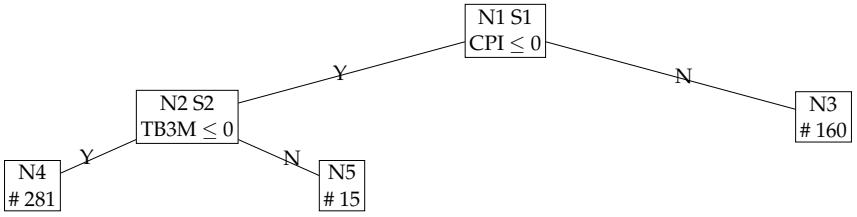


Figure 3: **The Tree Structure**

The figure illustrates the identified regimes using the entire monthly sample period from 1986 to 2023, showing the tree growth process. The algorithm splits based on inflation, then splits high/low interest rate periods into two regimes when inflation is low, resulting in three. These macro indicators are standardized by subtracting the previous 10-year rolling window average and then smoothing.

inflation), marked in red, covers events such as the Gulf War (1990-1991) and the early phase of the COVID-19 pandemic (2020); these periods are characterized by economic instability and rising prices, reflecting the high inflation environment.

Regime 2 (low inflation and low interest rates), shown in blue, encompasses events such as Black Monday (1987), the dissolution of the Soviet Union (1991), the Asian Financial Crisis (1997-1998), the 9/11 terrorist attacks (2001), the Lehman Brothers bankruptcy (2008), and the Brexit referendum (2016). This regime highlights periods of economic growth and stability with subdued inflation and interest rates, despite occasional financial disruptions.

Regime 3 (low inflation and high interest rates), highlighted in yellow, includes the official circulation of the Euro (2002) and the start of the Iraq War (2003). These events occurred during periods of low inflation but rising interest rates, often in response to geopolitical tensions and policy shifts. The figure also tracks US interest rates (dashed white line) and US Economic Policy Uncertainty (EPU) (solid black line), providing a visual correlation between these indicators and the economic regimes. Notably, spikes in EPU correspond with major events and transitions between regimes, indicating heightened economic uncertainty during these periods.

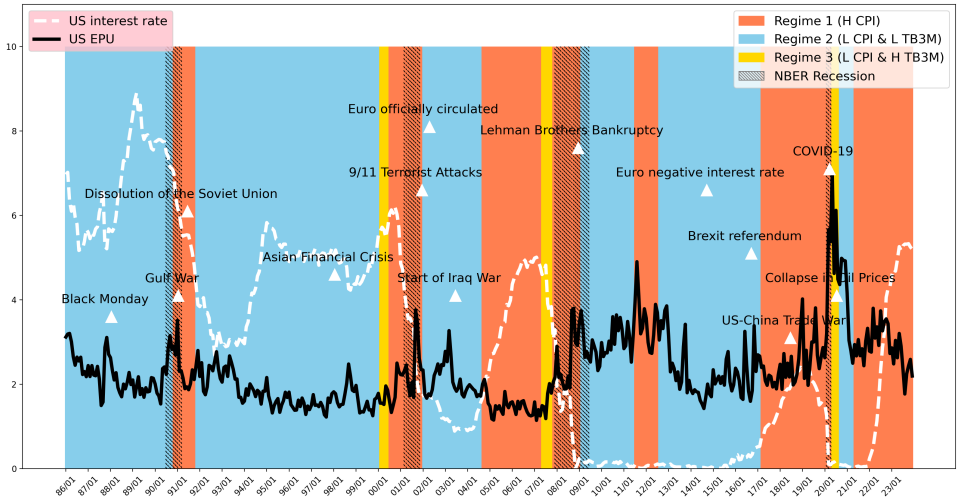


Figure 4: **Time Series Regimes**

The figure shows the detected regimes over time using the entire monthly sample from 1986 to 2023. Regime 1 (red) represents the high inflation regime, Regime 2 (blue) corresponds to the low inflation and low interest rate regime, and Regime 3 (yellow) represents the low inflation and high interest rate regime. The shaded areas represent NBER recession periods. Additionally, the figure includes time series of US interest rates, US EPU (https://www.policyuncertainty.com/), and several global events that affect the world economy.

4.3 US Macroeconomic Regimes and Factor Risk Premia

We have seen above that each regime features different macroeconomic conditions, suggesting that factor risk premia across regimes may differ. To this end, we examine the estimated factor risk premia for each regime using the three types of prior beliefs: the confident, agnostic, and skeptical priors. We summarize the posterior results from 2,000 MCMC sample draws and present the factor risk premia estimation for each regime in Table 4.

In Regime 1, characterized by high inflation, the Carry factor consistently exhibits high statistically significant positive risk premia for all priors, 0.42% for the confident prior, 0.44% for the agnostic prior, and 0.45% for the skeptical prior, indicating its robustness to inflation conditions. The MKT Beta factor also exhibits a significant positive risk premium, ranging from 0.62% for the skeptical prior to 0.65% for the confident prior, even higher than that of the Carry factor, reflecting the potential high profitability of the beta strategy in high inflation conditions. We also note that the risk

premium of the NFA factor is high for the three types of priors, ranging from 0.41% for the skeptical prior to 0.42% for the confident prior. Put together, the three factors of market beta, Carry, and NFA deliver statistically significant and economically substantial risk premia under a regime that features high inflation. In contrast, the risk premia of other factors, including the short-term momentum and value factors, are small and not statistically significant.

Regime 2 corresponds to periods of low inflation and low interest rates. We note that the Carry factor stands out with a high positive risk premium, ranging from 0.39% for the confident prior to 0.43% for the skeptical prior. Those factor risk premia are smaller than the corresponding ones in Regime 1. However, we find that the factor risk premium of NFA is much smaller than that in Regime 1 and only statistically significant for the confident prior, and the factor risk premium of market beta is not statistically significant for all three types of priors. We note that the value factor generates a statistically significant positive risk premium, ranging from 0.10% for the skeptical prior to 0.18% for the confident prior.

Regime 3, representing low inflation and high interest rates, shows a more complex landscape. The Carry factor continues to generate a statistically significant risk premium, but only for the confident prior, 0.35%, and for the agnostic and skeptical priors, its risk premium is only 0.24% and 0.13%, respectively. However, we find that in this regime, the volatility factor becomes more important and generates a high statistically significant factor risk premium for the confident and agnostic priors, 0.45% and 0.35%, respectively.

Table 5 presents the selection probabilities of factors under the detected regimes for three types of prior beliefs to further illustrate the strength of factors under various regimes. Consistent with the factor risk premium estimates, in Regime 1, the factors of Carry, NFA, and MKT Beta are all selected with a 100% probability for all three types of prior beliefs, underscoring their robustness in the high inflation environment.

In Regime 2, only the Carry factor is selected with a probability of 100% for the three types of priors. The value factor is selected with a probability larger than 90%

Table 4: **Factor Risk Premia under Various Regimes**

The table shows factor risk premia (%) estimation results for three identified regimes based on inflation and interest rate data (see Figure **??**). Regime 1 represents high inflation, Regime 2 corresponds to low inflation and low interest rates, and Regime 3 represents low inflation and high interest rates. Each regime group presents Risk premia estimates (with 5 % and 95 % credible intervals in the parentheses) based on prior selection probability (confident prior with $w = 0.9$, agnostic prior $w = 0.5$, and skeptic prior $w = 0.1$). The number is the mean (5 % and 95 % quantiles in the parentheses) of 2000 MCMC post-convergence samples of λ.

	Regime 1 (H CPI)			Regime 2 (L CPI & L TB3M)			Regime 3 (L CPI & H TB3M)		
Factors	w = 0.9	w = 0.5	w = 0.1	w = 0.9	w = 0.5	w = 0.1	w = 0.9	w = 0.5	w = 0.1
Carry	0.420 [0.30, 0.54]	0.438 [0.32, 0.55]	0.449 [0.35, 0.55]	0.386 [0.27, 0.50]	0.403 [0.29, 0.50]	0.427 [0.34, 0.52]	0.348 [0.01, 0.65]	0.244 [-0.02, 0.58]	0.129 [-0.03, 0.52]
MOM1	0.106 [-0.00, 0.23]	0.056 [-0.02, 0.19]	0.031 [-0.02, 0.08]	0.042 [-0.03, 0.14]	0.024 [-0.03, 0.08]	0.017 [-0.03, 0.06]	-0.141 [-0.47, 0.08]	-0.042 [-0.32, 0.05]	-0.004 [-0.06, 0.05]
MOM6	0.024 [-0.06, 0.15]	0.008 [-0.04, 0.06]	0.008 [-0.04, 0.05]	0.171 [0.03, 0.30]	0.079 [-0.01, 0.23]	0.033 [-0.02, 0.08]	0.057 [-0.35, 0.49]	0.039 [-0.06, 0.32]	0.012 [-0.05, 0.07]
MOM12	-0.058 [-0.20, 0.04]	-0.016 [-0.08, 0.04]	-0.009 [-0.05, 0.04]	-0.121 [-0.24, 0.00]	-0.041 [-0.19, 0.03]	-0.020 [-0.07, 0.03]	0.037 [-0.34, 0.44]	0.018 [-0.08, 0.24]	0.009 [-0.04, 0.06]
Value	-0.040 [-0.14, 0.03]	-0.017 [-0.07, 0.03]	-0.015 [-0.06, 0.03]	0.183 [0.10, 0.26]	0.163 [0.05, 0.25]	0.099 [0.02, 0.21]	-0.063 [-0.31, 0.11]	-0.028 [-0.22, 0.05]	-0.009 [-0.06, 0.04]
NFA	0.424 [0.31, 0.54]	0.413 [0.31, 0.53]	0.409 [0.31, 0.51]	0.157 [0.06, 0.25]	0.087 [0.00, 0.21]	0.034 [-0.01, 0.08]	0.158 [-0.08, 0.44]	0.091 [-0.04, 0.40]	0.017 [-0.05, 0.08]
LDC	0.063 [-0.02, 0.18]	0.029 [-0.03, 0.12]	0.021 [-0.03, 0.07]	-0.007 [-0.07, 0.05]	-0.002 [-0.05, 0.05]	-0.003 [-0.05, 0.04]	0.118 [-0.07, 0.41]	0.070 [-0.04, 0.36]	0.018 [-0.04, 0.07]
LT Yield	0.109 [-0.01, 0.25]	0.056 [-0.02, 0.21]	0.029 [-0.03, 0.09]	0.139 [0.02, 0.26]	0.076 [-0.01, 0.22]	0.030 [-0.02, 0.08]	-0.066 [-0.37, 0.18]	-0.005 [-0.13, 0.07]	0.002 [-0.05, 0.06]
Term Spread	-0.008 [-0.08, 0.06]	-0.005 [-0.06, 0.05]	-0.003 [-0.05, 0.04]	-0.041 [-0.14, 0.03]	-0.023 [-0.08, 0.03]	-0.017 [-0.06, 0.03]	0.200 [-0.08, 0.60]	0.131 [-0.04, 0.58]	0.059 [-0.04, 0.45]
Volatility	0.095 [-0.01, 0.22]	0.043 [-0.02, 0.17]	0.023 [-0.03, 0.07]	0.070 [-0.01, 0.16]	0.035 [-0.02, 0.12]	0.033 [-0.01, 0.08]	0.451 [0.19, 0.70]	0.349 [-0.00, 0.65]	0.167 [-0.02, 0.54]
MKT_Beta	0.651 [0.54, 0.77]	0.628 [0.52, 0.74]	0.620 [0.51, 0.73]	0.048 [-0.02, 0.14]	0.020 [-0.03, 0.07]	0.016 [-0.03, 0.06]	-0.019 [-0.26, 0.19]	-0.003 [-0.09, 0.07]	-0.001 [-0.05, 0.05]

Table 5: **Factor Selection Probability under Various Regimes**

The table shows risk premia selection results for three identified regimes based on inflation and interest rate data. Regime 1 represents high inflation, Regime 2 represents low inflation and low interest rates, and Regime 3 represents low inflation and high interest rates. Each regime group displays risk premia selection probabilities based on prior selection probabilities (confident prior with $w = 0.9$, agnostic prior $w = 0.5$, and skeptic prior $w = 0.1$). The numbers represent the mean of 2000 MCMC post-convergence samples of γ.

	Regime 1 (H CPI)			Regime 2 (L CPI & L TB3M)			Regime 3 (L CPI & H TB3M)		
Factors	w = 0.9	w = 0.5	w = 0.1	w = 0.9	w = 0.5	w = 0.1	w = 0.9	w = 0.5	w = 0.1
Carry	100	100	100	100	100	100	93	64	32
MOM1	75	26	3	47	10	1	73	22	3
MOM6	48	7	0	91	43	3	71	22	2
MOM12	56	10	1	82	21	1	70	22	1
Value	48	8	1	99	95	42	63	13	1
NFA	100	100	100	95	56	3	78	35	4
LDC	58	13	2	37	5	0	70	30	4
LT Yield	72	26	4	91	51	5	68	13	1
Term Spread	38	7	0	42	8	0	79	36	12
Volatility	68	18	1	59	11	2	99	84	37
MKT_Beta	100	100	100	53	8	1	59	15	2

for the confident and agnostic priors, and for the skeptical prior, its selection probability decreases to 42%. Other factors such as NFA, LT Yield, and MOM6 also have selection probabilities larger than 90% for the confident prior; however, their selection probabilities decrease drastically when we use less confident priors (i.e., agnostic and skeptical priors).

In Regime 3, none of the factors is selected with a 100% probability. However, we find that the factors of Carry and volatility are selected with a probability larger than 90% for the confident prior. For the agnostic prior, the volatility factor is selected with a probability of 84% and the Carry factor is selected with a probability of 64%, and the selection probability for the remaining factors is all lower than 50%. For the skeptical prior, all factors are selected with very small probabilities.

Similarly to what we have found in the previous subsection without regime switching, the Carry factor seems a strong and common factor, maintaining high selection probabilities irrespective of prior beliefs (except for the skeptical prior in regime 3); however, what differs is that its factor premium varies across three regimes. In con-

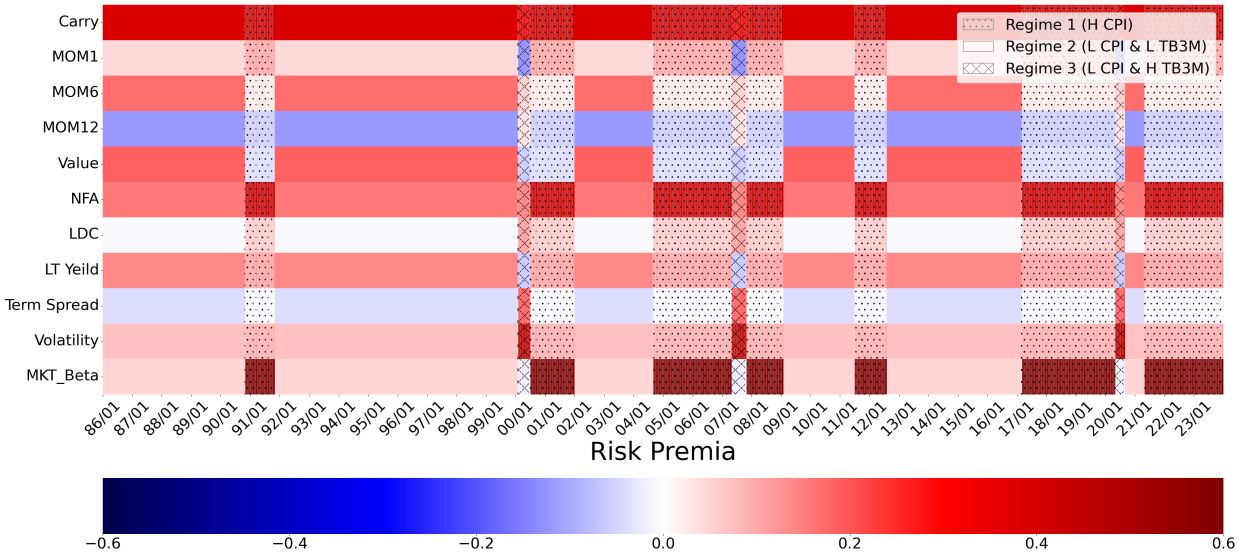


Figure 5: **Heatmap of Risk Premia in Time Series Regimes**

The figure shows the detected regimes over time using the entire monthly sample from 1986 to 2023 and the heatmap of risk premia estimate (%) under confident prior (w = 0.9). Regime 1 (red) represents the high inflation regime, Regime 2 (blue) corresponds to the low inflation and low interest rate regime, and Regime 3 (yellow) represents the low inflation and high interest rate regime.

trast, the other factors have regime-specific features and can be regarded as weak or uncommon. NFA and market beta factors become crucial in Regime 1, reflecting their sensitivity to high inflation. The value factor is important in the low inflation and low interest rate regime (Regime 2), followed by NFA, LT Yield, and MOM6 factors. The volatility factor gains prominence in the low inflation and high interest rate regime (Regime 3), reflecting its sensitivity to interest rate changes. Figure 5 presents the variation of the factor risk premia across regimes for the confident prior (w = 0.9) and clearly illustrates common/uncommon properties of the factors.

4.4 Mispricing and Idiosyncratic Volatility

The previous section suggests that currency risk premia shows variation across regimes. Given that our model allows for individual currency-specific α_i and σ_i, we evaluate the cross-sectional distributions of α and σ estimates to understand the evolution of potential mispricing and idiosyncratic volatility over regime shifting.

Table 6: **Cross-Sectional Alpha Estimation under Various Regimes**

The table displays estimation results for cross-sectional alpha distribution for three identified regimes based on inflation and interest rate data. Regime 1 indicates high inflation, Regime 2 corresponds to low inflation and low interest rates, and Regime 3 represents low inflation and high interest rates. Alpha estimates (%) are presented based on prior selection probability (confident prior with $w = 0.9$, agnostic prior $w = 0.5$, and skeptic prior $w = 0.1$) within each regime group. The cross-sectional average and standard deviation of the posterior mean of α estimates, calculated from 2000 MCMC post-convergence samples, and the 5th, 10th, 25th, median, 75th, 90th, and 95th percentiles are presented.

	Prior	Mean	Std	5%	10%	25%	Median	75%	90%	95%
Regime 1 (H CPI)	w = 0.9	-0.129	1.897	-0.331	-0.079	0.080	0.195	0.360	0.499	0.532
	w = 0.5	-0.125	1.898	-0.315	-0.083	0.073	0.185	0.368	0.489	0.542
	w = 0.1	-0.126	1.911	-0.301	-0.083	0.070	0.180	0.368	0.489	0.536
Regime 2 (L CPI & L TB3M)	w = 0.9	-0.036	0.527	-0.215	-0.140	-0.035	0.030	0.105	0.188	0.304
	w = 0.5	-0.026	0.520	-0.201	-0.130	-0.030	0.040	0.120	0.188	0.307
	w = 0.1	-0.013	0.512	-0.194	-0.124	-0.020	0.060	0.130	0.210	0.332
Regime 3 (L CPI & H TB3M)	w = 0.9	0.024	0.059	-0.059	-0.046	-0.005	0.020	0.060	0.108	0.110
	w = 0.5	0.030	0.056	-0.049	-0.038	-0.005	0.030	0.070	0.116	0.129
	w = 0.1	0.032	0.062	-0.049	-0.040	-0.010	0.020	0.085	0.116	0.138

Table 6 presents the estimated means of the cross-sectional alphas in the three distinct economic regimes discussed above. Panel (a) of Figure IA.2 estimates its kernel density. Regime 1, characterized by high inflation, shows significant negative mean alphas, about -0.13% for all three types of prior beliefs, which is in absolute value larger than the overall mispricing found in Table 3, suggesting the existence of substantial overpricing on average, which could be attributed to the restrictive monetary policy accompanying high inflation. However, while the 5% quantile is negative (-0.33% to -0.30%), the 95% quantile is highly positive (about 0.54%).

In contrast, Regime 3, characterized by low inflation and high interest rates, exhibits positive mean alpha values. This suggests that the market tends to underprice assets on average during periods of low inflation and high interest rates, possibly leading to investor overconfidence and increased investments in a high-interest-rate environment. For all three types of priors, the 5% quantile alpha is about -0.05%, and the

Table 7: **Cross-Sectional Idiosyncratic Volatility under Various Regimes**

The table shows posterior idiosyncratic standard deviation estimation results for three identified regimes based on inflation and interest rate data. Regime 1 represents high inflation, Regime 2 represents low inflation and low interest rates, and Regime 3 represents low inflation and high interest rates. Each regime group presents Risk premia selection probability based on prior selection probability (confident prior with $w = 0.9$, agnostic prior $w = 0.5$, and skeptic prior $w = 0.1$). The table includes the cross-sectional average and standard deviation of the posterior mean of σ estimates, calculated from 2000 MCMC post-convergence samples, and different percentiles.

	Prior	Mean	Std	5%	10%	25%	Median	75%	90%	95%
Regime 1 (H CPI)	w = 0.9	3.235	4.135	1.298	1.502	1.835	2.255	2.985	4.426	6.110
	w = 0.5	3.231	4.127	1.286	1.505	1.832	2.255	2.985	4.416	6.106
	w = 0.1	3.233	4.132	1.286	1.505	1.830	2.250	2.992	4.416	6.118
Regime 2 (L CPI & L TB3M)	w = 0.9	2.404	1.706	1.421	1.488	1.605	2.030	2.610	3.212	3.496
	w = 0.5	2.404	1.703	1.408	1.476	1.605	2.040	2.615	3.238	3.503
	w = 0.1	2.405	1.698	1.422	1.474	1.610	2.040	2.615	3.244	3.541
Regime 3 (L CPI & H TB3M)	w = 0.9	1.939	0.686	1.144	1.210	1.370	1.650	2.420	2.932	3.269
	w = 0.5	1.922	0.681	1.124	1.190	1.355	1.630	2.380	2.904	3.231
	w = 0.1	1.925	0.670	1.135	1.198	1.340	1.660	2.420	2.878	3.238

95% quantile alpha is about 0.13%. However, Regime 2, defined by low inflation and interest rates, features a slightly negative cross-sectional mean alpha, ranging from -0.013% for the skeptical prior to -0.036% for the confident prior, suggesting some extent of overpricing. The mispricing in regimes 2 and 3 is smaller than in Table 3.

Table 7 reports the estimated means of cross-sectional idiosyncratic volatility for the same economic regimes. Panel (b) of Figure IA.2 estimates its kernel density. In Regime 1, with high inflation, the mean idiosyncratic volatility is relatively high and consistent across all three types of priors, about 3.23%, with its 5% and 95% quantiles being 1.3% and 6.1%, respectively. This suggests that the currency-specific risk remains contained despite the adverse economic conditions, possibly due to widespread risk aversion and cautious investment strategies. The mean idiosyncratic volatility significantly decreases to a level of less than 2% for all three priors in Regime 3, which

features low inflation and high interest rates. This decreased idiosyncratic volatility reflects low market uncertainty and small currency-specific risks, likely due to high interest rate policies. The 5% and 95% quantiles are 1.1% and 3.2%, respectively. Regime 2, characterized by low inflation and interest rates, is a moderate period regarding idiosyncratic volatility, consistent with alpha estimates.

4.5 Connection to Structural Break Models

Our model is general and can be extended to a structural break model by simply modifying the split variable candidate. If we choose all calendar months to split instead of macro variables, the model becomes a structural break model where the identified split months are the breakpoints. In this case, the regimes are non-recurrent. Smith and Timmermann (2021) identify eight breaks in the full sample period. In that case, we restrict the number of breaks up to 8, resulting in nine distinct regimes.

Figure 6 presents the estimated break dates with the time series plots of the US Economic Policy Uncertainty (EPU) and interest rates from 1986 to 2023. We use different colors to represent distinct regimes, segmented by the identified structural break dates. Shaded areas indicate NBER recession periods. Figure IA.3 is the corresponding heatmap of risk premia estimation under confidence prior. Table IA.3 shows the risk premia estimation result and corresponding selection probability in parentheses. The first structural break aligns with the October 1987 stock market crash, known as Black Monday. This event causes a significant increase in economic uncertainty, as evidenced by a spike in the EPU index. The Federal Reserve responded by adjusting interest rates to stabilize the financial system. Short and medium momentum show positive premia, while long-term momentum's premium is negative. The second structural break corresponds with the onset of the Gulf War in January 1991 and the dissolution of the Soviet Union in December 1991. These two conflicts resulted in increased oil prices and heightened global economic uncertainty, leading to adjustments in interest rates and a noticeable impact on the EPU. The mid-term momentum effect is inverse during this period. Then a break happened before the Mexico Financial Crisis in early 1995. The Carry, long-term momentum, volatility and NFA show

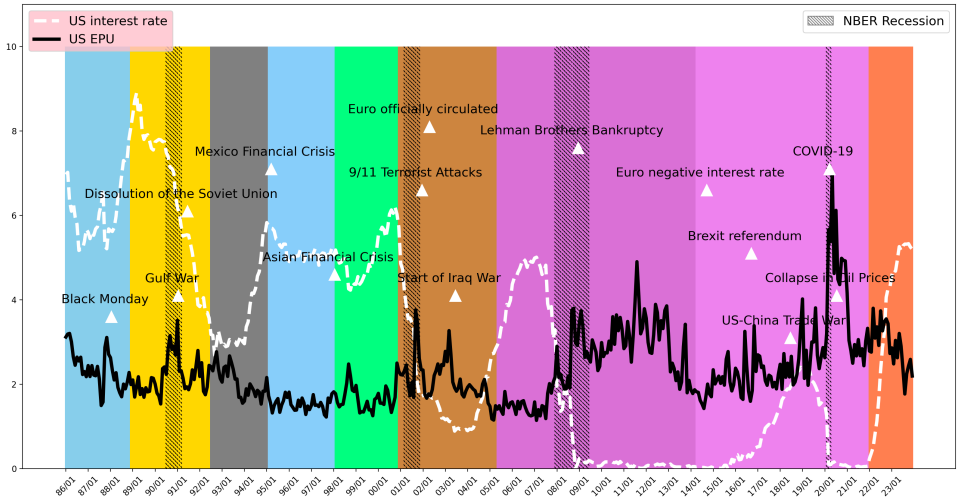


Figure 6: **Time Series Plot of Structural Break**

The figure shows estimated break dates using the entire monthly sample from 1986 to 2023, with different colors representing different regimes split by the break date points. Shaded areas represent NBER recession periods. The figure also includes a time series of US interest rates, the US EPU (https://www.policyuncertainty.com/), and global events that affect the world economy.

negative premia during this period.

The next break aligns with the Asian Financial Crisis, which began in July 1997. This crisis led to severe financial instability in Asian markets, causing global spillover effects that increased economic policy uncertainty and prompted changes in US interest rates. Notably, almost all factors show shrinkage in premia except for Carry. The next break happened in late 2000 before the 9/11 terrorist attacks. After that, the mid-term momentum shows negative premia while long-term momentum shows a strong premium. The period leading up to the Iraq War in March 2003 and before the 2008 global financial crisis saw another structural break. After this break, Carry, mid-term momentum, and MKT Beta show strong premia, while long-term momentum shows negative premium. Before the Euro's negative interest rate, another break happened. NFA and LT yield's premia increase a lot while long-term momentum remains negative. The onset of the COVID-19 pandemic is also during this period. The pandemic caused unprecedented global economic disruptions, spikes in EPU, and drastic monetary policy measures, including substantial interest rate cuts to mitigate the economic

fallout. After that, the economy recovered rapidly, and the interest rate increased, inducing the next break in early 2022. Carry, NFA, and MKT beta show strong risk premia, except for the short- and mid-term momentum, which show negative premia.

The structural break model effectively captures major events and institutional changes, but it may overlook the recurrent nature captured by macro variables. Regime-switching and structural break are mutually exclusive and exist simultaneously.

5 Conclusion

Macroeconomic dynamics can undergo significant shifts, often associated with financial crises or policy changes. This study presents a Bayesian regime-switching model to uncover currency risk-return relationships based on endogenously determined macroeconomic regimes. Exchange rate fluctuations have important impacts on aggregate demand, international trade, and the banking system, making it crucial to understand the underlying currency risk-return relationship for optimal exchange rate policy decisions.

Our model connects the dynamics of currency returns to currency characteristics in a panel regression model, with regime-specific mispricing, heteroskedasticity, and risk premia determined by macroeconomic variables. The model identifies macro-instrumented regimes, selects factors, and estimates risk premia specific to each regime, using a modified Bayesian spike-and-slab priors selection process validated by simulation. The growth of the decision tree is guided by the marginal likelihood improvement, accounting for both parameter and model uncertainties.

We identify three macroeconomic regimes based on inflation and interest rates: high inflation, low inflation, and low interest rates, and low inflation and high interest rates. Each regime has a unique risk premia structure, with the Carry factor being the most significant across regimes. This provides valuable insights for policymaking and evaluating their effects, and helps anticipate currency dynamics during interest rate adjustments, serving as a useful decision-making tool. Connecting with structural breaks, we can identify several breaks in currency risk premia that closely relate to

various global events.

References

Ang, A. and G. Bekaert (2002). International asset allocation with regime shifts. *Review of Financial Studies 15*(4), 1137–1187.

Ang, A. and J. Chen (2010). Yield curve predictors of foreign exchange returns. In *AFA 2011 Denver Meetings Paper*.

Asness, C., T. Moskowitz, and L. Pedersen (2013). Value and Momentum Everywhere. *Journal of Finance 68*, 929–985.

Avramov, D. (2002). Stock return predictability and model uncertainty. *Journal of Financial Economics 64*(3), 423–458.

Bekaert, G. (1995). The time variation of expected returns and volatility in foreign-exchange markets. *Journal of Business & Economic Statistics 13*(4), 397–408.

Bianchi, D., M. Büchner, and A. Tamoni (2021). Bond risk premiums with machine learning. *Review of Financial Studies 34*(2), 1046–1089.

Bryzgalova, S., J. Huang, and C. Julliard (2023). Bayesian solutions for the factor zoo: We just ran two quadrillion models. *Journal of Finance 78*(1), 487–557.

Chernov, M., M. Dahlquist, and L. A. Lochstoer (2023). Pricing Currency Risks. *Journal of Finance 78*, 693–730.

Chib, S. (1995). Marginal likelihood from the Gibbs output. *Journal of the American Statistical Association 90*(432), 1313–1321.

Chib, S. (1998). Estimation and comparison of multiple change-point models. *Journal of Econometrics 86*(2), 221–241.

Chipman, H. A., E. I. George, and R. E. McCulloch (2010). BART: Bayesian additive regression trees. *Annals of Applied Statistics 4*, 266–298.

Cimadomo, J., D. Giannone, M. Lenza, F. Monti, and A. Sokol (2022). Nowcasting with large Bayesian vector autoregressions. *Journal of Econometrics 231*(2), 500–519.

Colacito, R., S. Riddiough, and L. Sarno (2020). Business Cycles and Currency Returns. *Journal of Financial Economics 137*(3), 659–678.

Cong, L. W., G. Feng, J. He, and X. He (2023). Growing the Efficient Frontier on Panel Trees. Technical report, City University of Hong Kong.

Cong, L. W., G. Feng, J. He, and J. Li (2023). Sparse Modeling Under Grouped Heterogeneity with an Application to Asset Pricing. Technical report, National Bureau of Economic Research.

Creal, D. and J. Kim (2021). Empirical Asset Pricing with Bayesian Regression Trees. Technical report, University of Notre Dame.

Cui, L., G. Feng, Y. Hong, and J. Yang (2023). Time-Varying Factor Selection: A Sparse Fused GMM Approach. Technical report, City University of Hong Kong.

Dahlquist, M. and H. Hasseltoft (2020). Economic Momentum and Currency Returns. *Journal of Financial Economics 136*(1), 152–167.

Della Corte, P., T. Ramadorai, and L. Sarno (2016). Volatility Risk Premia and Exchange Rate Predictability. *Journal of Financial Economics 120*, 21–40.

Della Corte, P., S. J. Riddiough, and L. Sarno (2016). Currency Premia and Global Imbalances. *Review of Financial Studies 29*, 2161–2193.

Fama, E. F. and K. R. French (2020). Comparing cross-section and time-series factor models. *Review of Financial Studies 33*(5), 1891–1926.

Fan, Z., J. M. Londono, and X. Xiao (2022). Equity tail risk and currency risk premiums. *Journal of Financial Economics 143*(1), 484–503.

Feng, G. and J. He (2022). Factor investing: A Bayesian hierarchical approach. *Journal of Econometrics 230*(1), 183–200.

Frazzini, A. and L. H. Pedersen (2014). Betting against beta. *Journal of Financial Economics 111*(1), 1–25.

Freyberger, J., A. Neuhierl, and M. Weber (2020). Dissecting characteristics nonparametrically. *Review of Financial Studies 33*(5), 2326–2377.

Fulop, A. and J. Li (2013). Efficient learning via simulation: A marginalized resample-move approach. *Journal of Econometrics 176*(2), 146–161.

Gabaix, X. and M. Maggiori (2015). International Liquidity and Exchange Rate Dynamics. *Quarterly Journal of Economics 130*(3), 1369–1420.

George, E. I. and R. E. McCulloch (1993). Variable selection via Gibbs sampling. *Journal of the American Statistical Association 88*(423), 881–889.

Giannone, D., M. Lenza, and G. E. Primiceri (2021). Economic predictions with big data: The illusion of sparsity. *Econometrica 89*(5), 2409–2437.

Gu, S., B. Kelly, and D. Xiu (2020). Empirical asset pricing via machine learning. *Review of Financial Studies 33*(5), 2223–2273.

Hamilton, J. D. (1989). A new approach to the economic analysis of nonstationary time series and the business cycle. *Econometrica: Journal of the Econometric Society*, 357–384.

Hamilton, J. D. (2016). Macroeconomic regimes and regime shifts. *Handbook of Macroeconomics 2*, 163–201.

Hansen, B. E. (1999). Threshold effects in non-dynamic panels: Estimation, testing, and inference. *Journal of Econometrics 93*(2), 345–368.

Hansen, B. E. (2000). Sample splitting and threshold estimation. *Econometrica 68*(3), 575–603.

Hansen, B. E. and B. Seo (2002). Testing for two-regime threshold cointegration in vector error-correction models. *Journal of Econometrics 110*(2), 293–318.

Harvey, C. R. and G. Zhou (1990). Bayesian inference in asset pricing tests. *Journal of Financial Economics 26*(2), 221–254.

He, J. and P. R. Hahn (2023). Stochastic tree ensembles for regularized nonlinear regression. *Journal of the American Statistical Association 118*(541), 551–570.

He, J., S. Yalov, and P. R. Hahn (2019). XBART: Accelerated Bayesian additive regression trees. In *The 22nd International Conference on Artificial Intelligence and Statistics*, pp. 1130–1138.

Johnson, T. C. (2002). Volatility, momentum, and time-varying skewness in foreign exchange returns. *Journal of Business & Economic Statistics 20*(3), 390–411.

Kelly, B. T., S. Pruitt, and Y. Su (2019). Characteristics are covariances: A unified model of risk and return. *Journal of Financial Economics 134*(3), 501–524.

Kho, B.-C. (1996). Time-varying risk premia, volatility, and technical trading rule profits: Evidence from foreign currency futures markets. *Journal of Financial Economics 41*(2), 249–290.

Koijen, R. S., T. J. Moskowitz, L. H. Pedersen, and E. B. Vrugt (2018). Carry. *Journal of Financial Economics 127*(2), 197–225.

Kozak, S., S. Nagel, and S. Santosh (2020). Shrinking the cross-section. *Journal of Financial Economics 135*(2), 271–292.

Lettau, M., S. C. Ludvigson, and J. A. Wachter (2008). The declining equity premium: What role does macroeconomic risk play? *Review of Financial Studies 21*(4), 1653–1687.

Lettau, M., M. Maggiori, and M. Weber (2014). Conditional Risk Premia in Currency Markets and Other Asset Classes. *Journal of Financial Economics 114*, 197–225.

Li, J., L. Sarno, and G. Zinna (2024). Skewness risk premia and the cross-section of currency returns. *Working Paper*.

Liu, X. and R. Chen (2020). Threshold factor models for high-dimensional time series. *Journal of Econometrics 216*(1), 53–70.

Lustig, H., N. Roussanov, and A. Verdelhan (2011). Common risk factors in currency markets. *Review of Financial Studies 11*, 527–553.

Lustig, H., N. Roussanov, and A. Verdelhan (2014). Countercyclical Currency Risk Premia. *Journal of Financial Economics 11*, 527–553.

Lustig, H., A. Stathopoulos, and A. Verdelhan (2019). The term structure of currency carry trade risk premia. *American Economic Review 109*(12), 4142–4177.

Lustig, H. and A. Verdelhan (2007). The Cross Section of Foreign Currency Risk Premia and Consumption Growth Risk. *American Economic Review 97*, 89–117.

Massacci, D. (2017). Least squares estimation of large dimensional threshold factor models. *Journal of Econometrics 197*(1), 101–129.

Massacci, D. (2023). Testing for regime changes in portfolios with a large number of assets: A robust approach to factor heteroskedasticity. *Journal of Financial Econometrics 21*(2), 316–367.

McConnell, M. and G. Perez-Quiros (2000). Output Fluctuations in the United States: What has changed since the early 1980s. *American Economic Review 90*, 1464–1476.

Menkhoff, L., L. Sarno, M. Schmeling, and A. Schrimpf (2012a). Carry trades and global FX volatility. *Journal of Finance 67*, 681–718.

Menkhoff, L., L. Sarno, M. Schmeling, and A. Schrimpf (2012b). Currency Momentum Strategies. *Journal of Financial Economics 106*, 620–684.

Menkhoff, L., L. Sarno, M. Schmeling, and A. Schrimpf (2017). Currency Value. *Review of Financial Studies 30*, 416–441.

Nucera, F., L. Sarno, and G. Zinna (2024). Currency risk premiums redux. *Review of Financial Studies 37*(2), 356–408.

Pástor, L. and R. F. Stambaugh (2001). The equity premium and structural breaks. *Journal of Finance 56*(4), 1207–1239.

Pesaran, M. H. (2006). Estimation and inference in large heterogeneous panels with a multifactor error structure. *Econometrica 74*(4), 967–1012.

Smith, S. C. and A. Timmermann (2021). Break risk. *Review of Financial Studies 34*(4), 2045–2100.

Smith, S. C. and A. Timmermann (2022). Have risk premia vanished? *Journal of Financial Economics 145*(2), 553–576.

Stock, J. H. and M. W. Watson (1996). Evidence on structural instability in macroeconomic time series relations. *Journal of Business & Economic Statistics 14*(1), 11–30.

Appendix

A.I Derivation of Marginal Likelihood

For any model M, data y, and parameter vector θ, from Bayes rule:

$$p(y, \theta|M) = p(y|\theta, M)p(\theta|M) = p(\theta|y, M)p(y|M) \tag{A.1}$$

and thus

$$p(y|M) = \frac{p(y|\theta, M)p(\theta|M)}{p(\theta|y, M)} \tag{A.2}$$

Taking logs of both sides, we obtain

$$\ln p(y|M) = \ln p(y|\theta, M) + \ln p(\theta|M) - \ln p(\theta|y, M) \tag{A.3}$$

The log marginal likelihood on the left-hand side does not involve θ, and so the equation must hold for any value of θ. Thus, for purposes of computational reliability, let us choose a $\hat{\theta}$ of high posterior density:

$$\ln p(y|M) = \ln p(y|\hat{\theta}, M) + \ln p(\hat{\theta}|M) - \ln p(\hat{\theta}|y, M) \tag{A.4}$$

The first two terms on the right-hand side of the equality are readily available. That is, $\ln p(y|\hat{\theta}, M)$ is the log likelihood evaluated at $\hat{\theta}$ and $\ln p(\hat{\theta}|M)$ is the log prior ordinate at $\hat{\theta}$. The last term $\ln p(\hat{\theta}|y, M)$ requires more care, since the normalizing constant of the posterior is typically unknown. We can evaluate it from the Gibbs sampling output from Chib (1995).

Our parameter set $\theta = [\alpha, \lambda, \sigma, \gamma]$. First, write

$$p(\hat{\theta}|y) = p(\hat{\lambda}|\hat{\gamma}, \hat{\alpha}, \hat{\sigma}, y)p(\hat{\gamma}|\hat{\alpha}, \hat{\sigma}, y)p(\hat{\alpha}|\hat{\sigma}, y)p(\hat{\sigma}|y)$$

$p(\hat{\lambda}|\hat{\gamma}, \hat{\alpha}, \hat{\sigma}, y)$ is known, as it is simply an ordinate of the complete conditional for α,

for rest parameters approximate the density from R Gibbs samples:

$$
\begin{aligned}
p(\hat{\gamma}|\hat{\alpha},\hat{\sigma},y) &\approx \frac{1}{R}\sum_{r=1}^{R} p(\hat{\gamma}|\lambda^{(r)},\hat{\alpha},\hat{\sigma},y) \\
p(\hat{\alpha}|\hat{\sigma},y) &\approx \frac{1}{R}\sum_{r=1}^{R} p(\hat{\alpha}|\gamma^{(r)},\lambda^{(r)},\hat{\sigma},y) \\
p(\hat{\sigma}|y) &\approx \frac{1}{R}\sum_{r=1}^{R} p(\hat{\sigma}|\alpha^{(r)},\lambda^{(r)},\gamma^{(r)},y)
\end{aligned}
\tag{A.5}
$$

where $\hat{\alpha},\hat{\lambda},\hat{\gamma},\hat{\sigma}$ are the corresponding posterior mean from Gibbs output, and $\alpha^{(r)},\lambda^{(r)},\gamma^{(r)},\sigma^{(r)}$ are the r-th post-convergence Gibbs sample. Conditional posterior distributions are given in section 2.4.

A.II Early Stop Criterion and Further Split

To prevent overfitting, we consider the possibility of definitively stopping the splitting process at the current node and terminating the algorithm, which we call the *null split rule* option. If the current node does not split, all the data will stay in the same leaf node and fit one model. Therefore, the split criterion for the null split rule is

$$
l(\emptyset) = |\mathcal{C}|\left(\frac{(1+d)^{\tilde{a}_2}}{\tilde{a}_1} - 1\right) p(\mathbf{R} \mid \mathbf{Z}) = |\mathcal{C}|\left(\frac{(1+d)^{\tilde{a}_2}}{\tilde{a}_1} - 1\right) p(\mathcal{R}_0), \tag{A.6}
$$

where $|\mathcal{C}|$ is the total number of all candidates, and d is the depth of the current node. Note that the root node has a depth of 1, and nodes that are one extra level beneath it have one more depth. The extra term before the marginal likelihood controls the strength of the regularization of the tree size. Specifically, $\tilde{a}_1$ and $\tilde{a}_2$ are two prior hyperparameters for the tree shrinkage. Following the XBART framework of He et al. (2019) and He and Hahn (2023) and the BART of Chipman et al. (2010), we choose $\tilde{a}_1 = 0.95$ and $\tilde{a}_2 = 2$. Intuitively, as $\tilde{a}_2 = 2$, the penalty of growing the tree (adding one extra depth) increases exponentially with the current depth. Deeper nodes tend to stop, and thus, regularization plays a role.

After calculating the split criterion for all candidates and the stop option, we as-

sume that the prior probability of each option is proportional to 1. Therefore, the posterior of selecting one of them follows the Bayes rule as

$$L(c_j) = \frac{l(c_j)}{\sum_{j'} l(c_{j'}) + l(\emptyset)}, \quad L(\emptyset) = \frac{l(\emptyset)}{\sum_{j'} l(c_{j'}) + l(\emptyset)}. \tag{A.7}$$

Equation (A.7) guides the selection of the best option (either a split candidate or a stop option) at each iteration. The option that maximizes the criterion is chosen. The algorithm proceeds to the next split if the selected option is a split rule candidate. If it is the stop option, the current node ceases to split further, and the algorithm concludes.

The second split follows a similar process and can occur at the left or right child nodes resulting from the first split. The tree grows iteratively, considering split candidates for both nodes together. The set of candidates expands to $\mathcal{C} = c_k^{\mathcal{R}_1} \cup c_k^{\mathcal{R}_2}$, where the superscript indicates the node to be split.

Each candidate, whether at the root's left or right child nodes, generates two new leaf nodes, resulting in three. The joint marginal likelihood or split criterion, corresponding to Equation (6), is:

$$l(c_j^{\mathcal{R}_1}) = p(\mathcal{R}_3) \times p(\mathcal{R}_4) \times p(\mathcal{R}_2), \quad l(c_j^{\mathcal{R}_2}) \quad = p(\mathcal{R}_1) \times p(\mathcal{R}_5) \times p(\mathcal{R}_6). \tag{A.8}$$

The split criterion of the stop option is[3]

$$l(\emptyset^{\mathcal{R}_1}) = |\mathcal{C}| \left(\frac{(1+d)^{\tilde{a}_2}}{\tilde{a}_1} - 1 \right) p(\mathcal{R}_1) \times p(\mathcal{R}_2), \quad l(\emptyset^{\mathcal{R}_2}) \quad = |\mathcal{C}| \left(\frac{(1+d)^{\tilde{a}_2}}{\tilde{a}_1} - 1 \right) p(\mathcal{R}_2) \times p(\mathcal{R}_1),$$

where $\emptyset^{\mathcal{R}_1}$ and $\emptyset^{\mathcal{R}_2}$ denote the option of stopping split $\mathcal{R}_1$ or $\mathcal{R}_2$, respectively.

The calculation for all candidates in $\mathcal{C} = \{c_j^{\mathcal{R}_1}\} \cup \{c_j^{\mathcal{R}_2}\}$ and two stop options proceed similarly as in Equation (A.7),

$$\begin{aligned} W &= \sum_{j'} l(c_{j'}^{\mathcal{A}_1}) + \sum_{j'} l(c_{j'}^{\mathcal{A}_2}) + l(\emptyset^{\mathcal{A}_1}) + l(\emptyset^{\mathcal{A}_2}) \\ L(c_j^{\mathcal{A}_1}) &= \frac{l(c_j^{\mathcal{A}_1})}{W}, L(\emptyset^{\mathcal{A}_1}) = \frac{l(\emptyset^{\mathcal{A}_1})}{W}, L(c_j^{\mathcal{A}_2}) = \frac{l(c_j^{\mathcal{A}_2})}{W}, L(\emptyset^{\mathcal{A}_2}) = \frac{l(\emptyset^{\mathcal{A}_2})}{W}. \end{aligned} \tag{A.9}$$

[3] $d = 2$ for the second split, since nodes $\mathcal{R}_1$ or $\mathcal{R}_2$ has depth 2.

We select the option that maximizes Equation (A.9) as the second split. Unlike typical tree algorithms in machine learning that recursively define the split criterion based on data within the node, our criterion is defined *globally*. Equation (A.8) encompasses all resulting leaf nodes and the entire dataset. This approach prevents myopic local optimization and mitigates overfitting.

Internet Appendix

(Not for Publication)

IA.I Simulation

Our Gibbs sampler in section 2.4 uses a modified spike-and-slab prior, estimating alpha and idiosyncratic volatility for each individual, then estimating the same risk premia across cross section. Hence, this method differs from conventional approaches (such as George and McCulloch (1993)) that solely rely on sampling along a single dimension, disregarding the cross-sectional information. To test the validity of our method, we conduct a simulation. The cross section of asset returns resembles the empirical properties of 49 currencies. We consider $K = 10$ characteristics, $N = 50$ assets, and $T = 600$ time periods. Specifically, we consider three kinds of factors: strong factors, weak factors, and useless factors, where the strong factors have large risk premia, the weak factors have smaller risk premia, and the useless factors have no risk premia when generating data.

The data-generating process is as follows. First, we fix the risk premia of 10 factors at $\lambda = [0.5, 0.4, 0.2, 0.1, 0.07, 0.05, 0.02, 0.01, 0, 0]$, then the first three factors are strong, the following five factors are weak, while the last two factors are useless. For each individual currency i, we first simulate α_i, σ_i, and ten characteristics level $\bar{z}_i$

$$\begin{aligned} \alpha_i &\sim N(0, 0.01^2) \\ \sigma_i &\sim |N(0, 0.5^2)| \\ \bar{z}_i &\sim N(0, 0.5^2) \end{aligned} \tag{IA.1}$$

then at each time t, we cross setionally generate characteristics $z_{i,t}$,rank them to evenly distributed in $[-1, 1]$ and generate $\epsilon_{i,t}$.

$$\begin{aligned} \mathbf{z}_{i,t-1} &\sim N(\bar{z}_i, 0.1^2) \\ \epsilon_{i,t} &\sim N(0, \sigma_i^2) \end{aligned} \tag{IA.2}$$

By multiplying the factor loadings (characteristics) with the risk premia at time t, and adding the intercept and innovation, we get the simulated returns $R_{i,t}$ for time t.

$$R_{i,t} = \alpha_i + \sum_{i=1}^{K} \lambda_i \times z_{i,t-1} + \epsilon_{i,t} \tag{IA.3}$$

In total, we have 600 $\times$ 50 currency returns observations. Each run contains 2000 MCMC samples, and the posterior inference of selection probability is based on the sample average.

Table IA.1 reports posterior factor risk premia estimates and selection probabilities. We can see that factor risk premia are estimated accurately in this simulation study. These results validate our modified spike-and-slab Gibbs sampler. Regardless of the presence of strong, weak, useless or their combination, our methodology can effectively identify them through sampling. The selection probabilities for strong factors consistently concentrate around 1, and those for weak factors may vary between 0 and 1. However, the useless factors are consistently unselected with very low selection probabilities close to 0.

Table IA.1: **Simulation Results**

The table displays the simulation results for risk premia estimation and selection probability. The factor consists of 3 strong factors,5 weak factors, and the remaining useless factors. The number is the sample average of $\boldsymbol{\lambda}_k$ and $\boldsymbol{\gamma}_k (k = 1...16)$ from 2000 post-convergence MCMC samples.

	True Premia (%)	Estimated Premia (%)			Selection Probability (%)		
Factors		w = 0.9	w = 0.5	w = 0.1	w = 0.9	w = 0.5	w = 0.1
				Strong Factors			
Z1	0.5	0.413	0.411	0.41	100	100	100
Z2	0.4	0.327	0.327	0.325	100	100	100
Z3	0.2	0.14	0.14	0.142	97.3	97.9	98
				Weak Factors			
Z4	0.1	0.079	0.078	0.078	7.5	7.2	6.6
Z5	0.07	0.059	0.058	0.061	1.6	1.7	2.1
Z6	0.05	0.063	0.062	0.064	2.9	2.5	2.8
Z7	0.02	0.001	0.001	0.001	0.4	0.4	0.4
Z8	0.01	0.02	0.019	0.017	0.2	0.2	0.2
				Useless Factors			
Z9	0	-0.011	-0.013	-0.012	0.4	0.4	0.4
Z10	0	-0.007	-0.008	-0.007	0.5	0.5	0.5

IA.II Additional Tables and Figures

Table IA.2: **Description of Data Source**

The table displays the data source of currency characteristics. There are 11 currency characteristics in total (Carry trade, 1-, 6-, 12-month momentum, value, net foreign asset, liabilities in domestic currency, long-term yield, term spread, volatility, and market beta). The monthly data sample spans from 1986 to 2023.

Characteristics	Calculation	Source
Carry	$(S_t - F_t)/S_t$	Authors' calculation based on spot and forward exchange rate quotes (midquote) from Barclays Bank International (BBI), Reuters and WM/Reuters accessed via Datastream.
MOM1	X_t	Authors' calculation based on spot and forward exchange rate quotes (midquote) from Barclays Bank International (BBI), Reuters and WM/Reuters accessed via Datastream.
MOM6	$X_{t-6:t}$	Authors' calculation based on spot and forward exchange rate quotes (midquote) from Barclays Bank International (BBI), Reuters and WM/Reuters accessed via Datastream.
MOM12	$X_{t-12:t}$	Authors' calculation based on spot and forward exchange rate quotes (midquote) from Barclays Bank International (BBI), Reuters and WM/Reuters accessed via Datastream.
Value	-($log(S_t/CPI_t) - log(S_{t-5yr}/CPI_{t-5yr})$)	CPI data is from IMF International Financial Statistics. Only for Taiwan CPI data come from National Statistics.
NFA	-(Total assets excl. gold-Total liabilities)/GDP (in US$)	The data are kindly provided by https://www.brookings.edu/articles/the-external-wealth-of-nations-database/.
LDC	Total liabilities * Exchange rate (end of period)	The data are kindly provided by https://www.brookings.edu/articles/the-external-wealth-of-nations-database/.
LT Yield	i_{10yr}	For the 10-year rates, we use the Long-term interest rates available on OECD Monthly Monetary and Financial Statistics.
Term Spread	$-(i_{10yr} - i_{3m})$	For the 10-year (3-month) rates, we use the Long (Short)-term interest rates available on OECD Monthly Monetary and Financial Statistics.
Volatility	$vol(r_{t-3m:t})$	The currency volatility is measured by the standard deviation of daily exchange rate return in the previous 3 months
MKT_Beta	β	The currency market beta is calculated by rolling 3-year regression of currency return on cross-sectional mean of currency return. We use negative beta in the empirical part following Frazzini and Pedersen (2014).

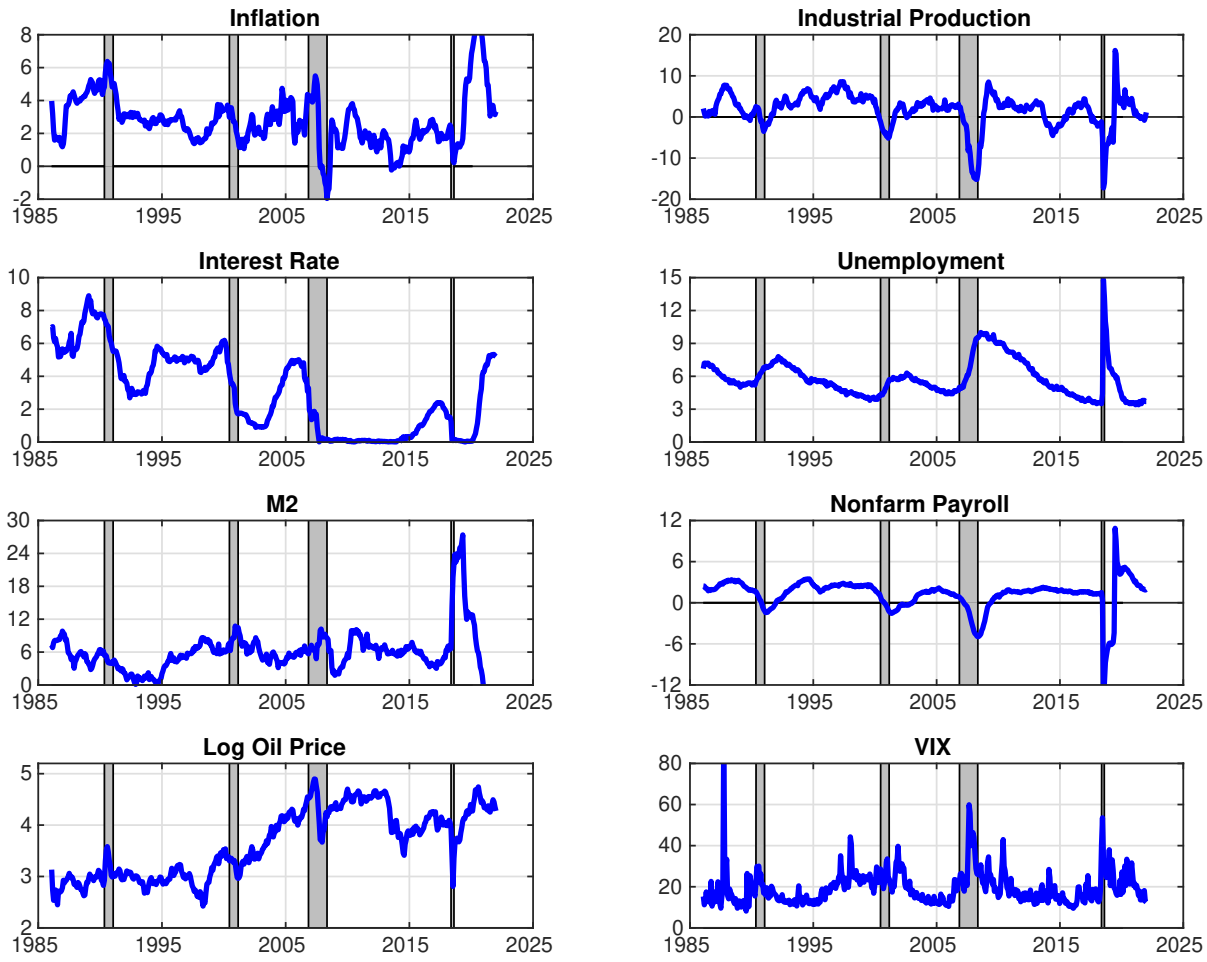
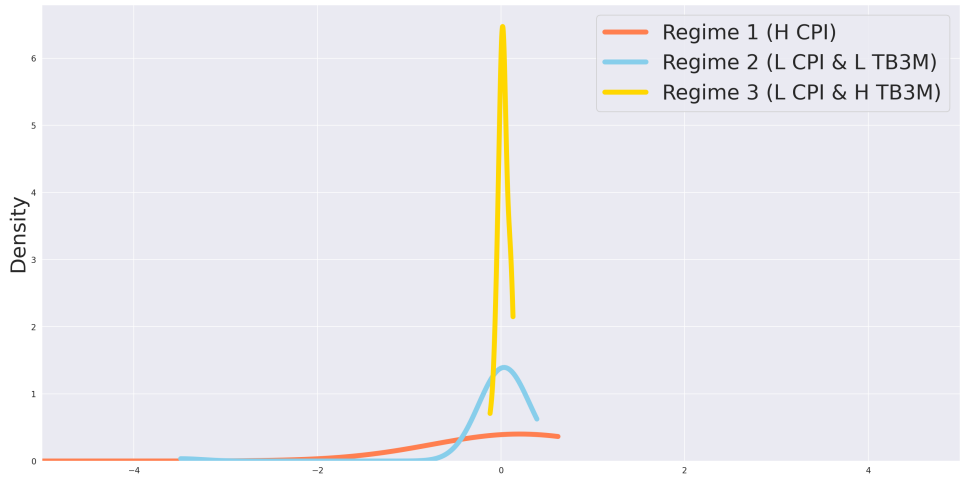
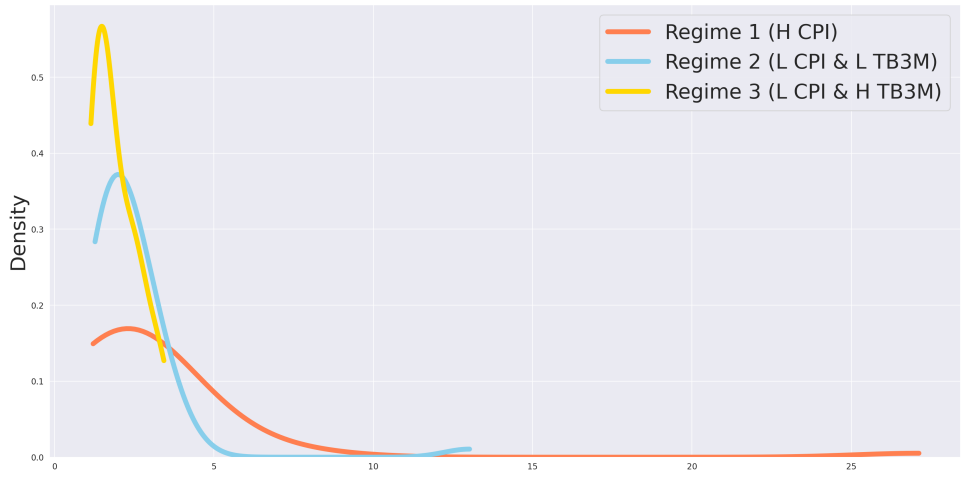


Figure IA.1: **Time-Series of Macro Variables**

The figure shows eight US macroeconomic indicators. Except for the crude oil price index, displayed on a logarithmic scale, the other variables are presented as annualized percentage changes. The shaded areas represent NBER recession periods. VIX is imputed by VXO in the early stage. The monthly data sample spans from January 1986 to December 2023.



(a) Alpha



(b) Sigma

Figure IA.2: **Cross-Sectional Alpha and Sigma distribution under Data-Driven Detected Regime**

The table displays cross-sectional alpha (panel (a)) and sigma (panel (b)) distribution estimation results for three regimes identified using the inflation and interest rate detected by data (see Figure 7) under confident prior (w = 0.9). The distribution is estimated using the kernel density estimate (KDE). Regime 1 represents the high inflation regime, Regime 2 corresponds to the low inflation and low interest rate regime, and Regime 3 represents the low inflation and high interest rate regime. The monthly sample spans from 1986 to 2023.

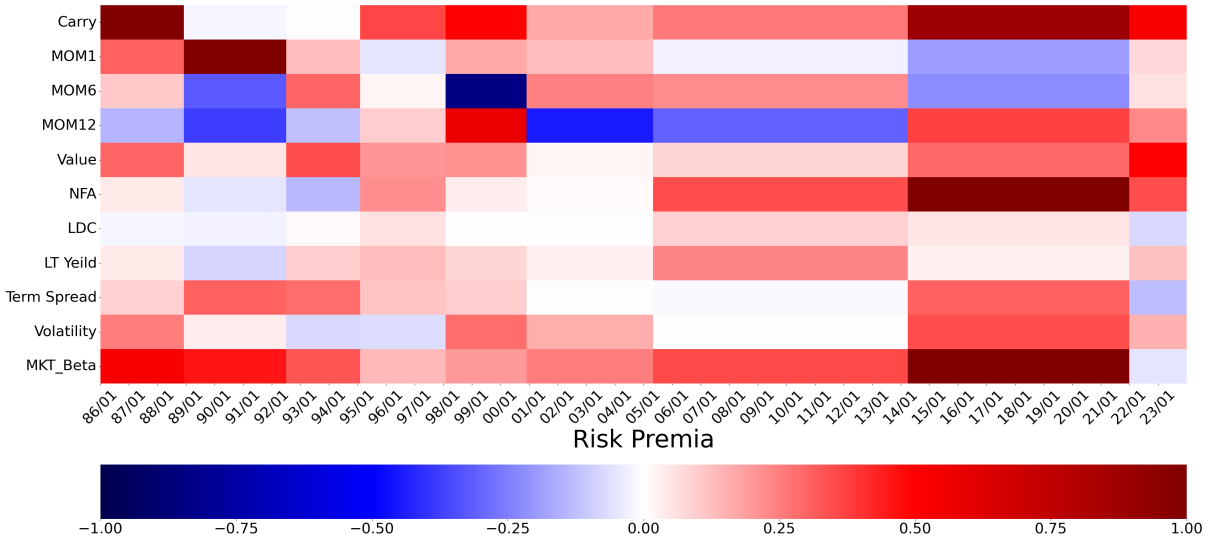


Figure IA.3: **Heatmap of Risk Premia Under Structual Break**

The figure presents the detected regimes (see Figure 6) over time using the entire monthly sample from 1986 to 2023 and the heatmap of risk premia estimate (%) under confident prior (w = 0.9). The regimes are identified by calendar month break (see Figure 6).

Table IA.3: **Factor Risk Premia and Selection under Structural Breaks**

The table displays risk premia estimation (%) and selection probability(%, in parentheses) estimation results for ten regimes identified by calendar month break (see Figure 6). Each regime group presents Risk premia estimates based on prior selection probability (confident prior with $w = 0.9$, agnostic prior $w = 0.5$, and skeptic prior $w = 0.1$). The number is the mean of 2000 MCMC post-convergence samples of λ and γ (in parentheses). The monthly sample spans from 1986 to 2023.

Date	1986-01 to 1988-11			1988-12 to 1992-06			1992-07 to 1995-01			1995-02 to 1998-01			1998-02 to 2000-11		
Factors	w = 0.9	w = 0.5	w = 0.1	w = 0.9	w = 0.5	w = 0.1	w = 0.9	w = 0.5	w = 0.1	w = 0.9	w = 0.5	w = 0.1	w = 0.9	w = 0.5	w = 0.1
Carry	0.524 (91)	0.291 (49)	0.010 (3)	1.011 (99)	0.984 (99)	0.724 (76)	-0.022 (71)	-0.051 (26)	-0.034 (7)	-0.006 (70)	0.049 (25)	0.018 (4)	0.364 (90)	0.487 (87)	0.465 (76)
MOM1	0.074 (75)	0.021 (26)	0.001 (2)	0.308 (86)	0.125 (37)	0.024 (5)	1.192 (99)	1.114 (99)	0.632 (68)	0.129 (72)	0.050 (24)	0.011 (2)	-0.052 (61)	-0.014 (15)	-0.003 (1)
MOM6	0.060 (77)	0.057 (28)	0.007 (3)	0.106 (75)	0.031 (21)	0.005 (2)	-0.324 (85)	-0.231 (50)	-0.085 (14)	0.303 (86)	0.156 (44)	0.020 (4)	0.019 (65)	0.011 (14)	0.006 (1)
MOM12	0.227 (81)	0.101 (32)	0.014 (4)	-0.147 (74)	-0.036 (22)	-0.007 (3)	-0.381 (87)	-0.296 (58)	-0.130 (21)	-0.121 (72)	-0.022 (19)	0.000 (2)	0.101 (69)	0.027 (17)	0.010 (2)
Value	0.507 (90)	0.254 (49)	0.009 (2)	0.297 (84)	0.267 (50)	0.201 (30)	0.049 (75)	0.056 (28)	0.040 (8)	0.345 (92)	0.202 (56)	0.042 (9)	0.206 (84)	0.065 (27)	0.017 (4)
NFA	0.351 (87)	0.255 (54)	0.098 (18)	0.039 (66)	0.007 (17)	0.003 (2)	-0.047 (68)	-0.022 (18)	-0.007 (2)	-0.139 (73)	-0.058 (25)	-0.023 (5)	0.225 (87)	0.117 (44)	0.035 (8)
LDC	-0.075 (70)	-0.033 (20)	-0.007 (2)	-0.017 (63)	-0.012 (16)	-0.005 (2)	-0.031 (69)	-0.028 (20)	-0.008 (2)	0.009 (61)	-0.025 (18)	-0.016 (3)	0.059 (61)	0.028 (16)	0.013 (2)
LT Yield	0.120 (79)	0.014 (24)	-0.002 (2)	0.043 (71)	0.013 (21)	0.004 (2)	-0.083 (71)	-0.024 (20)	-0.006 (2)	0.095 (72)	0.047 (24)	0.009 (2)	0.129 (72)	0.042 (22)	0.011 (3)
Term Spread	-0.127 (74)	-0.059 (26)	-0.012 (3)	0.090 (69)	0.023 (19)	0.001 (2)	0.308 (85)	0.118 (35)	0.015 (4)	0.283 (86)	0.124 (40)	0.024 (5)	0.111 (76)	0.087 (31)	0.044 (9)
Volatility	0.153 (81)	0.077 (31)	0.008 (2)	0.255 (81)	0.147 (40)	0.062 (11)	0.037 (67)	0.019 (19)	0.007 (2)	-0.074 (65)	-0.048 (23)	-0.018 (4)	-0.070 (61)	-0.037 (19)	-0.018 (3)
MKT_Beta	-0.054 (66)	-0.013 (17)	-0.003 (2)	0.529 (92)	0.459 (71)	0.318 (43)	0.455 (92)	0.419 (79)	0.247 (41)	0.333 (94)	0.213 (62)	0.029 (7)	0.136 (74)	0.046 (22)	0.014 (3)

Date	2000-12 to 2005-04			2005-05 to 2014-03			2014-04 to 2021-12			2022-01 to 2023-12		
Factors	w = 0.9	w = 0.5	w = 0.1	w = 0.9	w = 0.5	w = 0.1	w = 0.9	w = 0.5	w = 0.1	w = 0.9	w = 0.5	w = 0.1
Carry	0.494 (99)	0.564 (99)	0.635 (99)	0.171 (91)	0.133 (63)	0.062 (17)	0.263 (99)	0.265 (93)	0.264 (78)	0.889 (100)	0.939 (100)	0.924 (100)
MOM1	0.168 (80)	0.070 (30)	0.024 (5)	0.129 (83)	0.076 (38)	0.041 (9)	-0.025 (44)	-0.009 (8)	-0.006 (0)	-0.195 (79)	-0.084 (31)	-0.020 (4)
MOM6	-0.837 (99)	-0.786 (99)	-0.513 (73)	0.247 (98)	0.256 (92)	0.248 (81)	0.224 (96)	0.163 (68)	0.029 (6)	-0.220 (80)	-0.085 (30)	-0.021 (4)
MOM12	0.579 (99)	0.563 (93)	0.371 (58)	-0.449 (100)	-0.434 (100)	-0.402 (99)	-0.311 (99)	-0.278 (93)	-0.099 (32)	0.371 (91)	0.108 (35)	0.006 (2)
Value	0.212 (89)	0.148 (58)	0.051 (13)	0.022 (42)	0.012 (7)	0.012 (1)	0.085 (69)	0.040 (20)	0.026 (2)	0.292 (86)	0.134 (38)	0.042 (9)
NFA	0.038 (56)	0.002 (11)	-0.006 (1)	0.012 (43)	-0.003 (7)	-0.006 (0)	0.344 (99)	0.358 (99)	0.377 (99)	1.929 (100)	1.919 (100)	1.860 (100)
LDC	0.007 (51)	-0.001 (10)	-0.002 (1)	-0.001 (39)	-0.001 (6)	0.000 (0)	0.090 (71)	0.046 (22)	0.029 (3)	0.053 (61)	0.029 (17)	0.014 (3)
LT Yield	0.083 (64)	0.024 (15)	0.010 (1)	0.029 (50)	0.024 (14)	0.022 (2)	0.241 (97)	0.223 (84)	0.159 (47)	0.027 (66)	-0.009 (18)	-0.005 (2)
Term Spread	0.095 (67)	0.034 (19)	0.011 (2)	-0.004 (42)	0.002 (7)	0.006 (0)	-0.008 (41)	-0.005 (7)	-0.007 (1)	0.308 (90)	0.125 (39)	0.018 (4)
Volatility	0.285 (96)	0.204 (69)	0.090 (24)	0.163 (89)	0.079 (38)	0.022 (2)	0.004 (41)	0.002 (6)	0.000 (0)	0.346 (90)	0.294 (68)	0.136 (29)
MKT_Beta	0.196 (83)	0.065 (28)	0.012 (3)	0.257 (98)	0.155 (64)	0.045 (10)	0.358 (99)	0.341 (99)	0.284 (89)	1.636 (100)	1.538 (100)	1.414 (100)